

HIGH EFFICIENCY ISOLATED THREE
PORT DC-DC CONVERTER FOR DC
CHARGER STATIONS

AHMAD REDZUAN BIN ABDUL RAZAK

BACHELOR OF ELECTRICAL
ENGINEERING WITH HONOURS

UNIVERSITI MALAYSIA PAHANG

UNIVERSITI MALAYSIA PAHANG

DECLARATION OF THESIS AND COPYRIGHT

Author's Full Name : AHMAD REDZUAN BIN ABDUL RAZAK

Date of Birth : 26 AUGUST 1996

Title : HIGH EFFICIENCY ISOLATED THREE PORT DC-DC
CONVERTER FOR DC CHARGER STATIONS

Academic Session : SEMESTER II 2021/2022

I declare that this thesis is classified as:

- CONFIDENTIAL (Contains confidential information under the Official Secret Act 1997)*
- RESTRICTED (Contains restricted information as specified by the organization where research was done)*
- OPEN ACCESS I agree that my thesis to be published as online open access (Full Text)

I acknowledge that Universiti Malaysia Pahang reserves the following rights:

1. The Thesis is the Property of Universiti Malaysia Pahang
2. The Library of Universiti Malaysia Pahang has the right to make copies of the thesis for the purpose of research only.
3. The Library has the right to make copies of the thesis for academic exchange.

Certified by:



(Student's Signature)

960826-06-5125

Date: 15 JULY 2022



(Supervisor's Signature)

DR SULIANA AB GHANI

Date: 15 JULY 2022

NOTE: * If the thesis is CONFIDENTIAL or RESTRICTED, please attach a thesis declaration letter.

THESIS DECLARATION LETTER (OPTIONAL)

Librarian,
Perpustakaan Universiti Malaysia Pahang,
Universiti Malaysia Pahang,
Lebuhraya Tun Razak,
26300, Gambang, Kuantan.

Dear Sir,

CLASSIFICATION OF THESIS AS RESTRICTED

Please be informed that the following thesis is classified as RESTRICTED for a period of three (3) years from the date of this letter. The reasons for this classification are as listed below.

Author's Name	Ahmad Redzuan Bin Abdul Razak
Thesis Title	High Efficiency Isolated Three Port DC-DC Converter for DC Charger Stations

Reasons	(i)
	(ii)
	(iii)

Thank you.

Yours faithfully,

(Supervisor's Signature)

Date: 15 JULY 2022

Stamp:

Note: This letter should be written by the supervisor, addressed to the Librarian, *Perpustakaan Universiti Malaysia Pahang* with its copy attached to the thesis.



SUPERVISOR'S DECLARATION

I hereby declare that I have checked this thesis and, in my opinion, this thesis is adequate in terms of scope and quality for the award of the Electrical Engineering with Honours.

A handwritten signature in black ink, appearing to read 'Suliana', is written above a horizontal line.

(Supervisor's Signature)

Full Name : DR SULIANA AB GHANI
Position : SENIOR LECTURER
Date : 15 JULY 2022

(Co-supervisor's Signature)

Full Name :
Position :
Date :



STUDENT'S DECLARATION

I hereby declare that the work in this thesis is based on my original work except for quotations and citations which have been duly acknowledged. I also declare that it has not been previously or concurrently submitted for any other degree at Universiti Malaysia Pahang or any other institutions.

A handwritten signature in cursive script, appearing to read 'Ahmad', is written in black ink.

(Student's Signature)

Full Name : AHMAD REDZUAN BIN ABDUL RAZAK

ID Number : EC18050

Date : 15 JULY 2022

HIGH EFFICIENCY ISOLATED THREE PORT DC-DC CONVERTER
FOR DC CHARGER STATIONS

AHMAD REDZUAN BIN ABDUL RAZAK

Thesis submitted in fulfillment of the requirements
for the award of the
Bachelor of Electrical Engineering with Honours

College of Engineering
UNIVERSITI MALAYSIA PAHANG

DECEMBER 2022

ACKNOWLEDGEMENTS

First and foremost I would like thanks to God (Allah), for helping me to complete this thesis. I would like to express my sincere appreciation and gratitude to my supervisor, Dr Suliana Ab Ghani, lecturer of Electrical Department, Universiti Malaysia Pahang, for her supervision, guidance, encouragement, support and helpful discussions during completing this thesis.

I also want to wish my grateful thanks to my Final Year Project (FYP) coordinator, Dr Nur Huda Binti Ramlan due to his excellent organization of the online submission, as well as the progress between me and my supervisor and the presenting schedule, has successfully eliminated superfluous work for students and supervisors, particularly during the COVID19 pandemic.

Lastly, I would like to express my sincere gratitude to my family for their support, mentally and financially throughout my study. Without their help, this research might not go as easily as planned.

ABSTRAK

Krisis tenaga dunia telah mengakibatkan pemanasan global dan perubahan iklim. Pertumbuhan tenaga yang boleh diperbaharui mampu mengatasi krisis tenaga. Salah satu teknologi tenaga yang boleh diperbaharui adalah kenderaan elektrik (EV) dimana permintaan untuk jualan EV semakin meningkat pada setiap tahun. Teknologi pengecasan perlu dipertingkatkan kerana pengecas arus ulang alik (AC) yang sedia ada mempunyai pengecasan yang perlahan dan terhad kepada aplikasi kecil. Selain itu, keselamatan pengguna dan peralatan juga perlu dititikberatkan kerana penukar ciri-ciri DC-DC yang sedia ada mempunyai isu keselamatan. Oleh itu, system pengecas DC 100kW jambatan aktif ganda (DAB) telah dibangunkan menggunakan perisian MATLAB/Simulink. Memandangkan pengecas EV berbilang port telah dibangunkan, DAB telah dikembangkan kepada tiga port pengecas EV DC, yang dikenali sebagai penukar DC-DC jambatan aktif tiga (TAB) telah ditubuhkan. TAB telah diperkenalkan untuk mengatasi konfigurasi kompleks penukar multiport sedia ada yang melibatkan peringkat penukaran berbilang. Kedua-dua DAB dan TAB dimodulasi menggunakan modulasi anjakan fasa tunggal (SPS) dan diuji di bawah pelbagai sudut anjakan fasa. Kemudian, kecekapan TAB dinilai di bawah beberapa system beban iaitu 25kW, 50kW, 75kW dan 100kW. Secara, keseluruhannya, TAB dengan system beban 100kW mempunyai kecekapan yang lebih tinggi berbanding dengan yang lain dengan menghasilkan 86%, manakala system dengan 75kW mempunyai kecekapan yang paling rendah iaitu 66%.

ABSTRACT

The world energy crisis resulting the global warming and climate change. The renewable energy growth is capable to overcome the energy crisis. One of the technology renewable energies is electric vehicle (EV) where the demand for EV sales has increased every year. The charging technology need to be improved due to the existing alternating current (AC) charger has slow charging and limited to the low application. Besides that, the safety of consumers and equipment should also be emphasized due to current non-isolated DC-DC converter have safety issue. Therefore, the 100kW DC charger system based on isolated dual active bridge (DAB) DC-DC converter have been developed using MATLAB/Simulink software. Since the multiport EV charger have been concerned, the DAB has been expanded to three ports EV DC charger, known as triple active bridge (TAB) DC-DC converter is established. The TAB is introduced to overcome the complex configuration of the existing multiport converter that involving multiple conversion stage. Both DAB and TAB are modulated using single-phase shift (SPS) modulation and tested under various of phase-shift angle. Then, the efficiency of TAB is evaluated under several load systems which 25kW, 50kW, 75kW and 100kW. In overall, the TAB with 100kW load system have the higher efficiency compared to others by producing 86%, while the system with 75kW have the lowest efficiency with 66%.

TABLE OF CONTENT

DECLARATION	
TITLE PAGE	
ACKNOWLEDGEMENTS	ii
ABSTRAK	iii
ABSTRACT	iv
TABLE OF CONTENT	v
LIST OF TABLES	viii
LIST OF FIGURES	ix
LIST OF SYMBOLS	xi
LIST OF ABBREVIATIONS	xii
CHAPTER 1 INTRODUCTION	1
1.1 Project Background	1
1.2 Problem Statement	4
1.3 Objective of the Project	4
1.4 Scope of the Project	4
1.5 Thesis Outlines	5
CHAPTER 2 LITERATURE REVIEW	6
2.1 Introduction	6
2.2 Development of Electric Vehicle	6
2.3 Type of Electric Vehicle Charger	7
2.3.1 AC charger	8

2.3.2	DC charger	8
2.4	Dual Active Bridge	12
2.5	Triple Active Bridge	13
2.6	Summary of the Literature Review	15
CHAPTER 3 METHODOLOGY		16
3.1	Introduction	16
3.2	Flow Chart of the Project	16
3.3	Theoretical Calculation	18
3.3.1	DAB system	18
3.3.2	TAB System	19
3.4	Simulation Design of DAB	20
3.4.1	DAB Converter for Forward Direction	20
3.4.2	DAB Converter for Reverse Direction	21
3.5	Simulation Design of TAB	23
3.5.1	TAB Converter	23
CHAPTER 4 RESULTS AND DISCUSSION		26
4.1	Introduction	26
4.2	Simulation Results for Dual Active Bridge System	26
4.2.1	Results for DAB in Forward Direction	26
4.2.2	Results for DAB in Reverse Direction	28
4.3	Simulation Results for Triple Active Bridge System	29
4.3.1	100 kW TAB System	29
4.3.2	75 kW TAB System	32
4.3.3	50 kW TAB System	35

4.3.4	25 kW TAB System	37
4.4	Efficiency of the system	40
4.4.1	100 kW TAB System	40
4.4.2	75 kW TAB System	40
4.5	Discussion	41
CHAPTER 5 CONCLUSION		42
5.1	Conclusion	42
5.2	Recommendation	42
REFERENCES		44
APPENDIX A		48
APPENDIX B		49

LIST OF TABLES

Table 3.1 Parameters for DAB system	18
Table 3.2 Parameters for TAB system	19
Table 4.1 Result of the 100 kW TAB system (same phase-shift angle at the output side)	29
Table 4.2 Result of the 100 kW TAB system (different phase-shift angle at the output side)	31
Table 4.3 Result of the 75 kW TAB system (same phase shift angle at the output side)	32
Table 4.4 Result of the 75 kW TAB system (different phase-shift angle at the output side)	33
Table 4.5 Result of the 50 kW TAB system (same phase-shift angle at the output side)	35
Table 4.6 Result of the 50 kW TAB system (different phase-shift angle at the output side)	36
Table 4.7 Result of the 25 kW TAB system (same phase-shift angle at the output side)	37
Table 4.8 Result of the 25 kW TAB system (different phase-shift angle at the output side)	39

LIST OF FIGURES

Figure 1.1 Percentage of conventional car used	1
Figure 1.2 Dual active bridge	3
Figure 1.3 Triple Active Bridge	3
Figure 2.1 Electric car of Belgian Camille Jenatzy, 1899	7
Figure 2.2 Block diagram of on-board charger	8
Figure 2.3 Block diagram of unidirectional and bidirectional power flow	9
Figure 2.4 Unidirectional full bridge	10
Figure 2.5 Non-isolated bidirectional charger	11
Figure 2.6 Isolated bidirectional dual active bridge charger	11
Figure 2.7 Dual active bridge configuration	13
Figure 2.8 Triple Active Bridge configuration	14
Figure 2.9 Summary of the literature for the project	15
Figure 3.1 Flowchart of the project	17
Figure 3.2 DAB converter for forward direction	21
Figure 3.3 DAB converter reverse direction	21
Figure 3.4 Pulse generator setting for primary side	22
Figure 3.5 Pulse generator setting for secondary side	23
Figure 3.6 One-input-two-output configuration	24
Figure 3.7 Two-input-one-output configuration	24
Figure 3.8 TAB converter circuit	25
Figure 4.1 Voltage pulse at primary and secondary side in forward direction	27
Figure 4.2 Output voltage and output current for forward circuit at 90°	27
Figure 4.3 Primary and secondary voltage	28
Figure 4.4 Output voltage and output current for reverse direction	29
Figure 4.5 Output voltage and current for 100kW with $0^\circ:90^\circ:90^\circ$	30
Figure 4.6 Output voltage and current for 100kW with $0^\circ:90^\circ:45^\circ$	32
Figure 4.7 Output voltage and current for 75kW with $0^\circ:40^\circ:40^\circ$	33
Figure 4.8 Output voltage and current for 75kW with with $0^\circ:40^\circ:10^\circ$	34
Figure 4.9 Output voltage and current for 50 kW with $0^\circ:25^\circ:25^\circ$	36
Figure 4.10 Output voltage and current for 50kW with $0^\circ:25^\circ:5^\circ$	37
Figure 4.11 Output voltage and current for 25kW with $0^\circ:11^\circ:11^\circ$	38
Figure 4.12 Output voltage and current for 25kW with $0^\circ:11^\circ:2^\circ$	39
Figure 4.13 Efficiency of 100 kW system	40

LIST OF SYMBOLS

θ	Phase angle
π	Phi
$^{\circ}$	Degree
rads	Radian
n	Transformer ratio
f_{sw}	Switching frequency
L_k	Leakage inductor
P_{out}	Output power
V_{in}	Input voltage
V_{out}	Output voltage
I_{in}	Input current
I_{out}	Output current
P1	Port 1
P2	Port 2
P3	Port 3

LIST OF ABBREVIATIONS

AC	Alternating Current
BEV	Battery Electric Vehicle
BMS	Battery Management System
DAB	Dual Active Bridge
DC	Direct Current
DPS	Double/Dual Phase Shift
EPS	Expanded Phase Shift
EV	Electric Vehicle
FCEV	Fuel Cell Electric Vehicle
HEV	Hybrid Electric Vehicle
HF	High Frequency
ICE	Internal Combustion Engine
IES	Integration Energy Storage
PHEV	Plug-in Hybrid Electric Vehicle
PSM	Phase Shift Modulation
RE	Renewable Energy
SEPIC	Single-Ended Primary-Inductor Converter
SPS	Single Phase Shift
TAB	Triple Active Bridge
THD	Total Harmonic Distortion
TPS	Triple Phase Shift
V2G	Vehicle To Grid
ZVS	Zero Voltage Switching

CHAPTER 1

INTRODUCTION

1.1 Project Background

World energy crisis with the technological advancements, greenhouse gas emissions have grown in recent years which resulting in global warming and climate change. One of the energy crisis happen is because of increasing of the conventional automobiles used [1]. The pie chart in Figure 1 shows that the conventional car user is higher than hybrid car and electric car with 94.2%. From the highest usage of the conventional automobile, it will contribute to the higher gas emission and air pollution will harming the environment and human life. These automobile demand will continue to grow every year due to the number of consumers and economic growth [2].

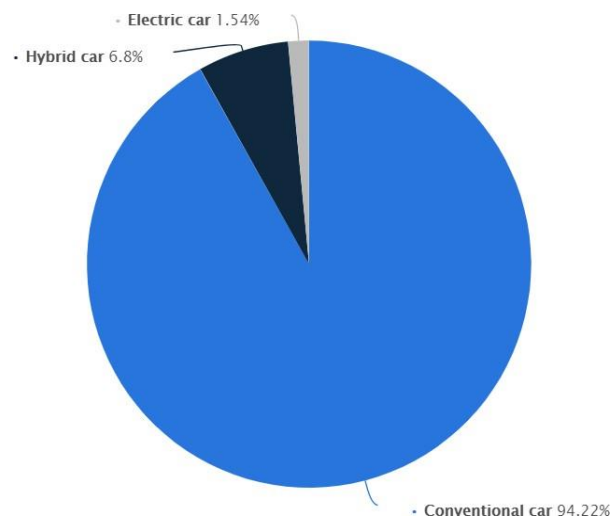


Figure 1.1 Percentage of conventional car used

Source: Joschka Muller (2022)

Energy is the most important factor for sustainability of the world. Global energy demand is growing every day, and non-renewable energy sources are now meeting many of it. Non-renewable energy sources are restricted, and their excessive usage has a

negative impact on the environment [3]. To overcome this crisis, renewable energy (RE) is introduced [4]. RE are gaining attention nowadays such as solar and wind turbine. RE have a few advantages like pollution free, clean energy and environment friendly. In order to support clean energy, the electric vehicle (EV) is introduced.

In recent years, the worldwide EV industry has been quickly expanding as a result of significant price reductions and the benefits of great energy efficiency and zero emissions [5]. EVs can accomplish greater power alteration efficiency, less exhaust radiations, and vibration, as compared to internal combustion engine (ICE). EV are a more environmentally friendly, cost-effective alternative and produce green energy compared to ICE. The growth of EV resulting the high demand of EV charger station.

One of the EV technology is vehicle to grid (V2G) technology [6], [7]. In V2G, it guarantees that it has a feature like bidirectional power flow [8]. For example, in V2G the grid can charge the EV and during shortage time the system in EV can supply back the power to the grid. There are two types of chargers of EV. First is Alternating Current (AC) charger known as on-board, it is for the low application and second is Direct Current (DC) charger known as off-board, so it usually uses for the high-power application.

Since DC charger have a high power, it can charge the EV faster compare to the AC charger [9]. This project will only focus on DC-DC converter. The DC-DC converter that have an advantages of bidirectional power flow, high power density and galvanic isolation is Dual Active Bridge (DAB). As stated in [10] DAB have two bridge which is primary bridge and secondary bridge as shown in Figure 1.2.

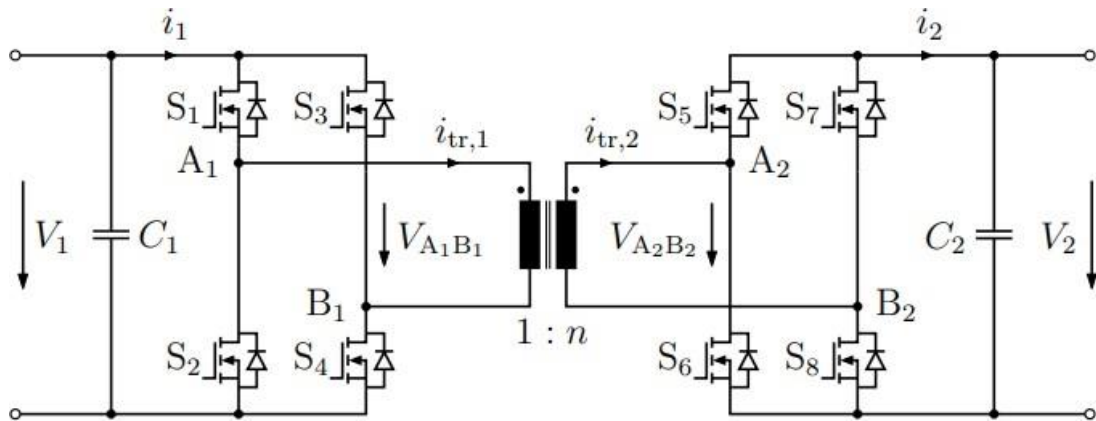


Figure 1.2 Dual active bridge
 Source: F. Krismer (2005)

Next, one of the advantages DABs is easy to cascade. From the DAB, the Triple Active Bridge (TAB) is easy to develop from the basic DAB. TAB have a three-port which is port-one can act as supply or source and the other port-two and port-three act as load. The Figure 1.3 show the configuration of TAB which is use for energy storage as state in this paper [11].

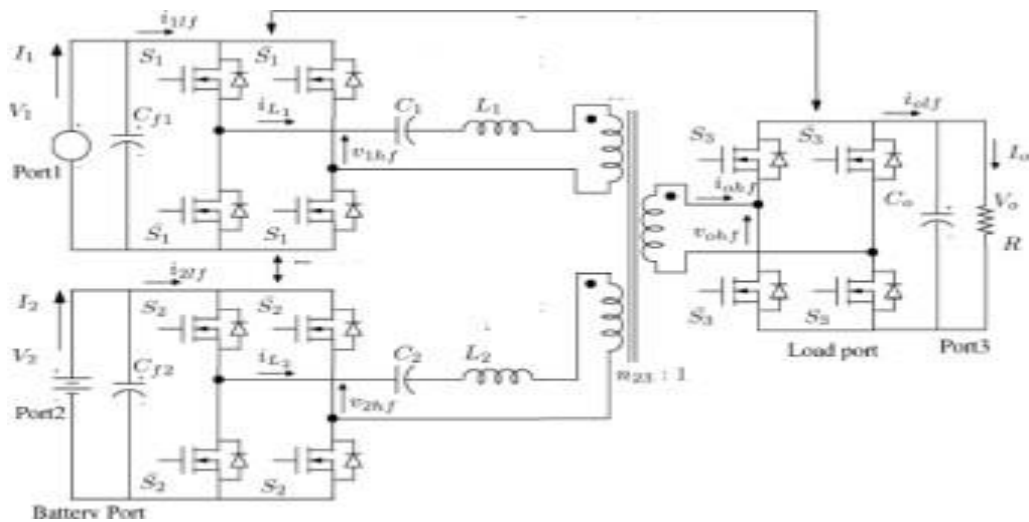


Figure 1.3 Triple Active Bridge
 Source: V Jeyarthikha (2014)

1.2 Problem Statement

The development of a dependable, efficient, and high-power density charger has become a major problem as EV technologies evolve. Components, control, and switching technique are all critical to its operation. However, at this moment the existing AC chargers have a slow charging time and limit to low application [9]. It will take a longer time for fully charging. After that, non-isolated DC-DC converter have issue in safety [12]. It is because, between the input and output, there is an electrical connection in the non-isolated DC-DC converter. Besides, the existing multiport is complex due to the multiple conversion stage [13]. It will have high phase current total harmonic distortion (THD), making it inconvenient.

1.3 Objective of the Project

The main objectives of this project are:

1. To design two-ports EV DC charger using bidirectional dual active bridge (DAB) DC-DC converter.
2. To develop three-ports EV DC charger using triple active bridge (TAB) DC-DC converter.
3. To evaluate the efficiency performance of TAB for various phase-shift angle and load system.

1.4 Scope of the Project

Along with the study, there are a few areas that are fixed to ensure the objectives can be achieved perfectly. The scopes for this project are

1. Design of DAB circuit using 100 kW by using MATLAB/Simulink software.
2. Use single phase shift (SPS) as phase shift modulation (PSM).
3. By using multi-winding transformer, the DAB circuit is improved to TAB circuit.

4. The system has been tested and evaluated for different phase shift angle under various load systems in open loop mode.

1.5 Thesis Outlines

This thesis is organized into five chapters:

- Chapter 1 provides the overview of the research which include the project background, problem statement, objective, and scope.
- Chapter 2 discussed the literature review on the technology of electric vehicle (EV).
- Chapter 3 describes the design of the electric vehicle (EV) charger in detail. This chapter also provide the detail on simulation.
- Chapter 4 presents the results that obtained in simulation.
- Chapter 5 concludes the simulation, which the author will state the outcome based on the result and discussion.

CHAPTER 2

LITERATURE REVIEW

2.1 Introduction

This chapter reviews the development, types, and charger in electric vehicle (EV) applications. Then, the overview, operation principle and advantages of DAB and TAB converter are discussed.

2.2 Development of Electric Vehicle

An electric vehicle is a car that is partially or entirely powered by electricity. Prior to the invention of cars with internal combustion engines, vehicles fitted with an electric motor were constructed. The original versions, built between 1830 and 1840, were clunky and unstable devices that travelled at a relatively slow speed. The period from the late 19th century to the beginning of the 20th century may be described as an electromobility boom. During this time, electric car manufacturing has been established in Europe and the United States.

Electric car production in the United States had reached 10,000 units by the turn of the century, and their number is many times more than that of gasoline vehicles. In 1899, an electric automobile broke beyond the 100 km/h barrier. This historic occurrence occurred in the French town of Asher, near Paris. Camille Jenatzy, a Belgian, set the record for electric vehicles. The car's body was made of aluminium alloy and tungsten.

It resembled the torpedo that had been put in the chassis. The electric vehicle's body was exposed. It was powered by two motors and weighed around a tonne. The electric vehicle attained a top speed of 105.88 kilometres per hour. Electric cars built in the late 19th century are shown in Figure 2.1.



Figure 2.1 Electric car of Belgian Camille Jenatzy, 1899

Source: Dennis David (2013)

In this modern era, electric vehicle is widely used in Europe, North & Central America, and Asia. It is because of the concerns about the environment and sustainable energy. It also has attracted the attentions of governments, industries, and customers. The environmental friendliness and lack of pollutants, the lightweight automobile, the lower cost, and the inexpensive fuel (electricity) are all advantages of the electric vehicle. The automobile costs seven to ten thousand dollars, which is three times less than the cost of filling, making it the most cost-effective option [14].

The availability and convenience of electric vehicle charging infrastructure are major variables influencing the future development and popularity of electric vehicles. There are several types of electric cars which are Battery Electric Vehicle (BEV), Hybrid Electric Vehicle (HEV), Plug-in Hybrid Electric Vehicle (PHEV) and Fuel Cell Electric Vehicle (FCEV). Next, the electric vehicles can be charging with two type of charger which are AC charger and DC charger.

2.3 Type of Electric Vehicle Charger

Electric Vehicles (EVs) have been offered as a better option to replace conventional vehicles, which is gathering a lot of traction. For electric vehicle, there are two charging methods which are AC charging and DC charging. On-board and off-board EV battery chargers with unidirectional or bidirectional power flow are available. The

EV's on-board AC-DC converter provides single-phase and three-phase AC power for charging. Meanwhile, DC charging is accomplished by giving direct DC power to the EV's battery using off-board AC-DC converter supplies.

2.3.1 AC charger

The usage of on-board chargers will undoubtedly improve the vehicle's charging accessibility. In contrast to off-board chargers, on-board chargers are built into EVs and allow charging in practically any location. As long as a single-phase and three-phase power source is available. The downside of this design is that an extra DC-AC inverter is required, as well as space and weight constraints. Figure 2.2 shows the block diagram of on-board charger.

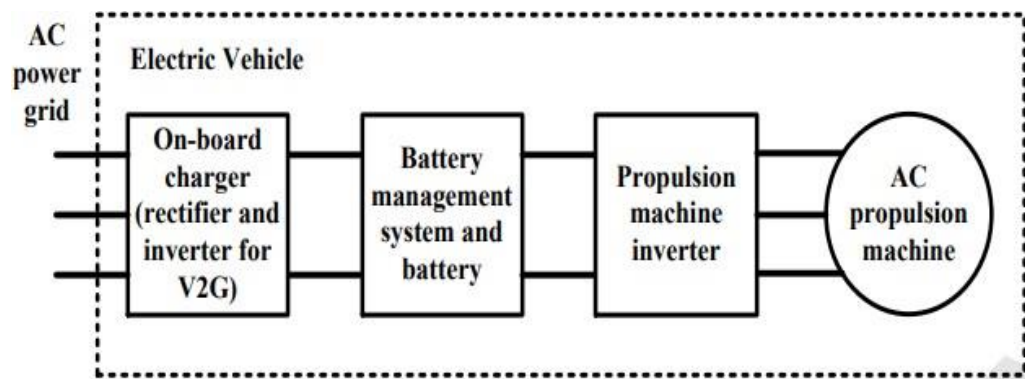


Figure 2.2 Block diagram of on-board charger

Source: K. Anusha (2020)

Because of weight, space, and cost limits, typical on-board chargers limit high power [15]. On-board chargers can be either conductive or inductive. Direct contact between the connection and the charge intake is used in conductive charging systems [16].

2.3.2 DC charger

The main of this project will be focus on DC charger due to the advantages. The DC chargers enable the use of higher-rated circuits. As a result, charging is completed in a shorter amount of time. It is offered as an outside unit rather than as part of the EV. A common DC charger can provide a greater DC voltage. As a result, the internal battery management system (BMS) must be capable of charging the battery by delivering this

voltage. EV Dc chargers can be classified as off-board with unidirectional or bidirectional power flow. An off-board battery charger is less restricted in terms of size and weight.

2.3.2.1 Unidirectional power flow

Between EVs and the electric grid, two modes of power flow are conceivable. Figure 2.3 shows the block diagram of basic unidirectional and bidirectional power flow. Unidirectional is a single power flow direction. Unidirectional chargers allow electric vehicles to charge but not to inject energy into the power grid. A diode bridge, a filter, and dc–dc converters are commonly used in these chargers.

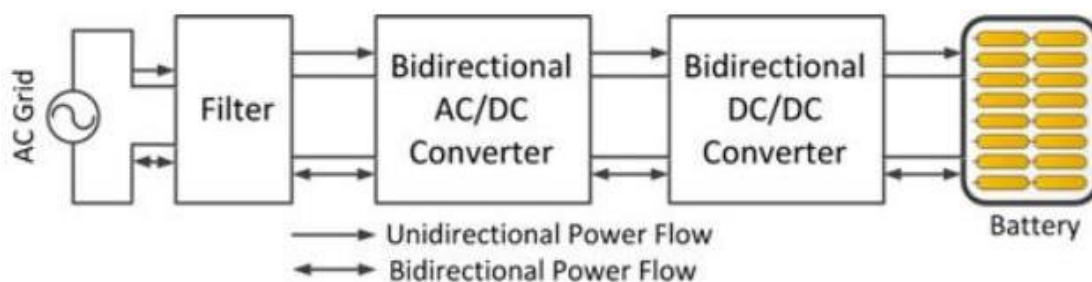


Figure 2.3 Block diagram of unidirectional and bidirectional power flow

Source: Dr L Ashok kumar (2020)

To decrease cost, weight, volume, and losses, these converters are now integrated in a single step [17]. When high-frequency isolation transformers are required, they can be used [18], [19]. Unidirectional charging is an obvious initial step since it reduces hardware needs, simplifies connector concerns, and reduces battery deterioration. Figure 2.4 presents an on-board unidirectional full-bridge series resonant charger for Level 1 systems (3.3 kW) similar in [19].

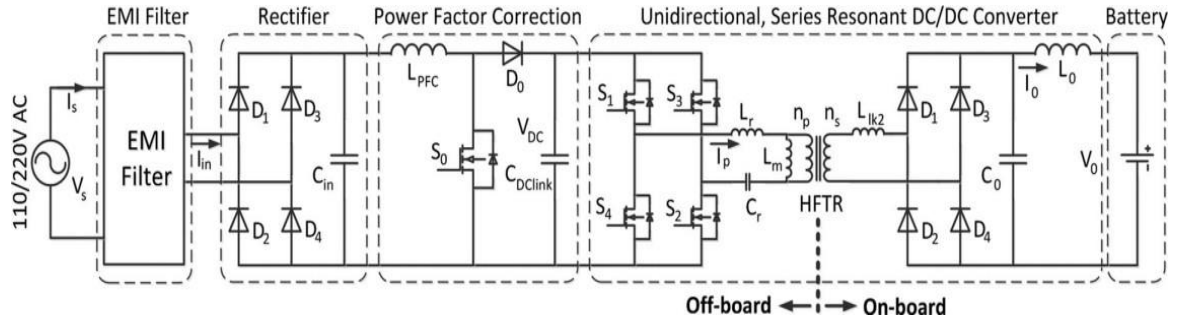


Figure 2.4 Unidirectional full bridge

Source: G. Choe (2010)

Due to the general simplicity of unidirectional charging control, a utility may manage severely loaded feeders caused to many EVs relatively easily [20]. Those with active front ends can use current phase angle control to offer local reactive power supply without needing to drain a battery. Unidirectional charging research aims to find the best charging schemes that maximise advantages while also investigating the influence on distribution networks [20], [21]. Unidirectional chargers can achieve most utility objectives while avoiding the expense, performance, and safety problems associated with bidirectional chargers, thanks to a high penetration of electric vehicles and active regulation of charging current [7].

2.4.1.1 Bidirectional power flow

A bidirectional charging system allows for grid charge, battery energy injection back into the grid, and power stability with proper power conversion [7]. An active grid connected bidirectional ac–dc converter enforces power factor, and a bidirectional dc–dc converter regulates battery current in a conventional bidirectional charger [19]. Non-isolated or isolated circuit topologies are available for these chargers.

To manage power and reactive power when operating in charge mode, they should draw a sinusoidal current with a set phase angle. The charger should return electricity in a sinusoidal pattern in discharge mode [7], [22], [23]. The vehicle-to-grid (V2G) operation mode of a bidirectional charger allows for charging from the grid, battery energy injection back to the grid, and power stabilisation [24]. Figure 2.5 displays the non-isolated bidirectional charger.

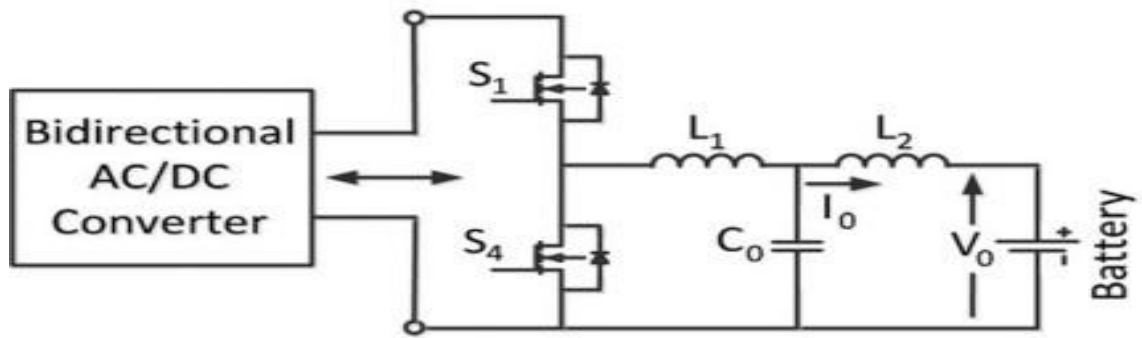


Figure 2.5 Non-isolated bidirectional charger
 Source: Jean-Michel Clairand (2018)

The control circuitry of this circuit is substantially simplified by the presence of two switches. However, there are two large and costly high-current inductors that can only buck in one direction and boost in the other [25]. The Figure 2.6 illustrates the isolated bidirectional dual active bridge (DAB) charger. The enormous number of components can contribute to the cost of this circuit, which delivers great power density and quick control [25].

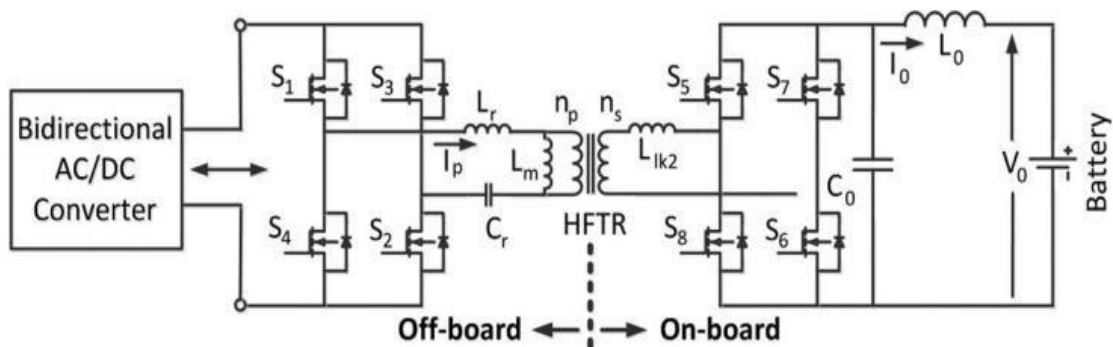


Figure 2.6 Isolated bidirectional dual active bridge charger
 Source: Jean_Michel Clairand (2018)

Battery deterioration caused to frequent cycling, the high cost of a charger with bidirectional power flow capabilities, metering concerns, and the need for distribution system changes are all obstacles that bidirectional power flow must overcome [26]. Other connectivity challenges, such as anti-islanding protection, must also be addressed. Chargers at levels 1, 2, and 3 can be unidirectional. Because Level 1 power constraints and cost objectives are modest, and it is critical to maximise flexibility, bidirectional chargers are only planned for Level 2 infrastructures. Reverse power flow is incompatible with the main aim and premise of Level 3 fast charging, which is to reduce connection

time and transfer significant energy as rapidly as feasible. There are several converters that have used bidirectional power flow which are non-isolated converter, isolated converter and dual active bridge converter.

2.4 Dual Active Bridge

This is especially fascinating given that DAB was founded many years ago, around 1990 [27]. Some of the applications in which DAB converter can be implemented. One of the applications is photovoltaic facility specifically is energy storage. The fundamental concept is to minimise the variation of the PV plant's power production in order to make grid control easier. DAB converter also of great usefulness in other applications which are vehicle to grid (V2G) and aerospace.

A DAB is defined by two active bridges coupled by a transformer that is often designed for high frequencies. One of the advantages DAB is the power-flow can be bidirectional because both bridges are operational. Bidirectional capabilities alone would not have led us to choose the DAB as our preferred converter, but galvanic isolation is particularly significant owing to safety considerations. By electrically isolating the battery, if a problem arises in the battery, the majority of electricity-related fatalities are reduced, at least in terms of human safety. Furthermore, when there is a power outage, the battery must release the previously stored energy to the grid. The DAB topology has been extensively investigated in a variety of contexts [28].

DAB consists of the DC voltage source, eight power switches S_1 – S_8 , capacitor, leakage inductor and transformer. DAB usually operated in such a mode that the switching frequency of S_1 - S_8 [29]. Operation of DAB interest on having in primary side operating 50% duty cycle. The power switches producing a VAB that is the voltage between the S_1 , and S_4 . The secondary side also toggled between S_5 and S_8 . Starting with input side S_1 , S_4 and secondary side S_5 , S_8 start a bit later. There is a phase shift between the primary side and secondary side [30] [31]. It is the control method for DAB by a phase-shift angle. There are several phase-shift control techniques for DAB converter which are single phase-shift (SPS), expanded phase-shift (EPS), triple phase-shift (TPS) and double or dual phase-shift (DPS). Figure 2.7 shows the DAB configuration. There

are several applications that used DAB such as in power supply application, hybrid vehicle, hybrid energy storage system and renewable energy.

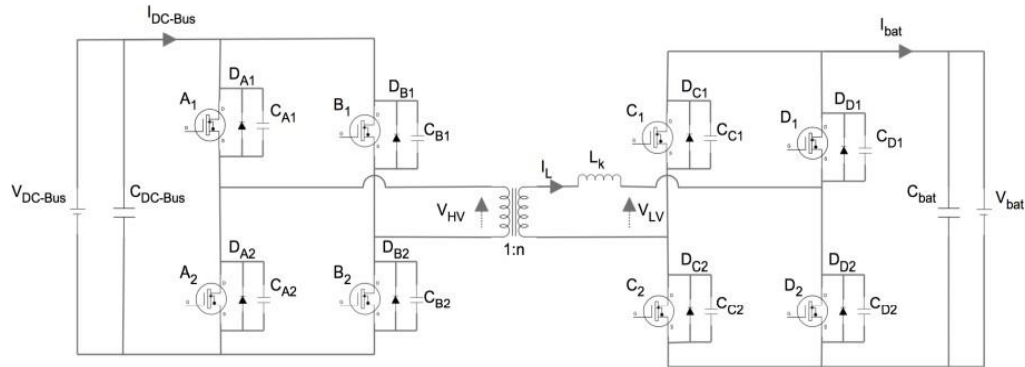


Figure 2.7 Dual active bridge configuration

Source: K. Sowjanya (2013)

2.5 Triple Active Bridge

A multiport converter is a self-sustaining multiple input/output static power converter that can interface with a variety of sources, storages, and loads [32]. A multiport converter combines many sources and may manage power flow and other capabilities using a control method. The converter is a more advanced form of a DAB-converter. To simplify the system, an integrated multi-port converter, which uses a single power conversion stage to interconnect all ports rather than multiple dc-dc conversion stages, can be implemented.

TAB has a three-port which is port-one can be act as supply or source and the other port, port-two and port-three can be act as load or vice versa. A two-stage bidirectional converter with three ports, a dc-dc converter between the source and the load, and a bidirectional dc-dc converter between the load and the source [33]. TAB can be design with one-input-two-load or two-load-one-input. The ports of TAB may have different power ratings and output voltage. The TAB converter is proposed for several applications in Integration Energy Storage (IES) and DC grid.

There are several advantages of TAB converter such as the flexibility to link sources with varying voltage ratings by modifying the HF transformer turn ratios, an integrated controller architecture, zero-voltage switching (ZVS) capabilities, and high-

power density. TAB converters also have the benefit of utilising a transformer, which not only converts the voltage ratio but also increases system safety. Aside from galvanic isolation, a significant benefit of this converter is the simplicity with which the varying voltage levels of the ports may be matched [33].

This converter has numerous working modes that affect the overall control system. The operation of TAB converter same as DAB converter by control the phase shifts and duty cycles. The power flow is controlled by the size of the phase angle, and the impedance of the circuit. Proper phase shifts of the voltages applied to the transformer windings can control the power flow [34]. Figure 2.8 shows the TAB configuration. The phase shifts determine the power flow between the three ports. Mostly TAB is used in the renewable energy, energy storage and load system.

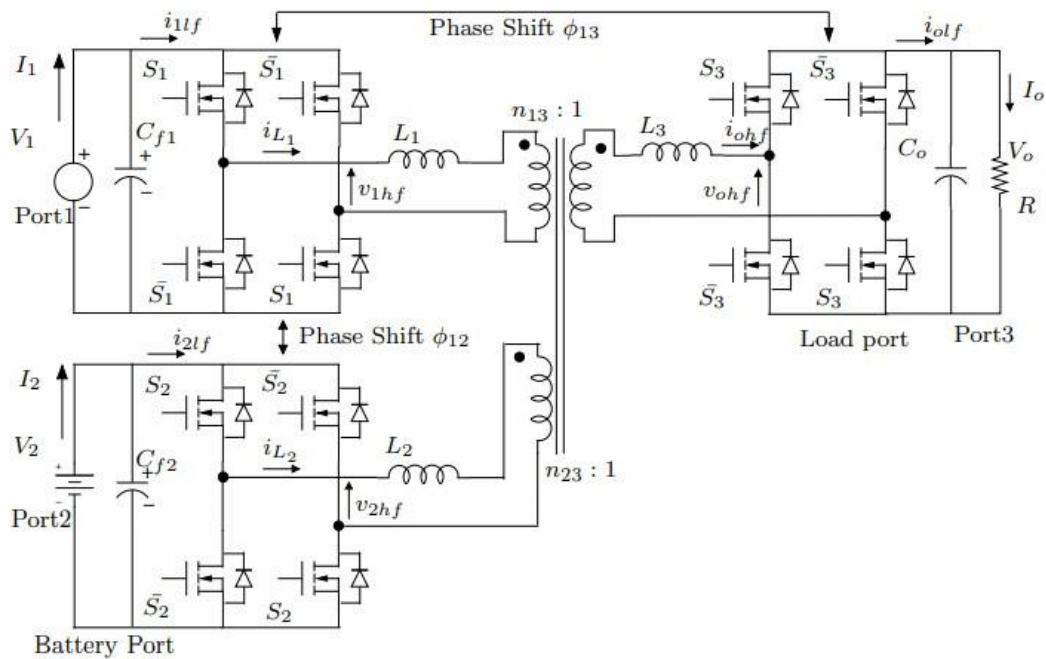


Figure 2.8 Triple Active Bridge configuration

Source: M. Michon (2004)

2.6 Summary of the Literature Review

Since the AC charger is used for the low power applications which is slow charging, this project will only focus on high power applications which use only DC charger. In DC charger, it has a DC-DC converter which divided into two types, unidirectional and bidirectional. Unidirectional only have one way direction of power flow meanwhile the bidirectional have two ways of direction power flow. In bidirectional, it has two types of circuit which are non-isolated and isolated. For the isolated type, it has a few types such as CUK, single-ended primary-inductor converter (SEPIC) and DAB. This project only focuses on DAB due to its advantages. From the DAB due to the have feature easy to cascade, the DAB will expand into TAB configuration. Figure 2.9 shows the graphical summary of substantial literature in this research work.

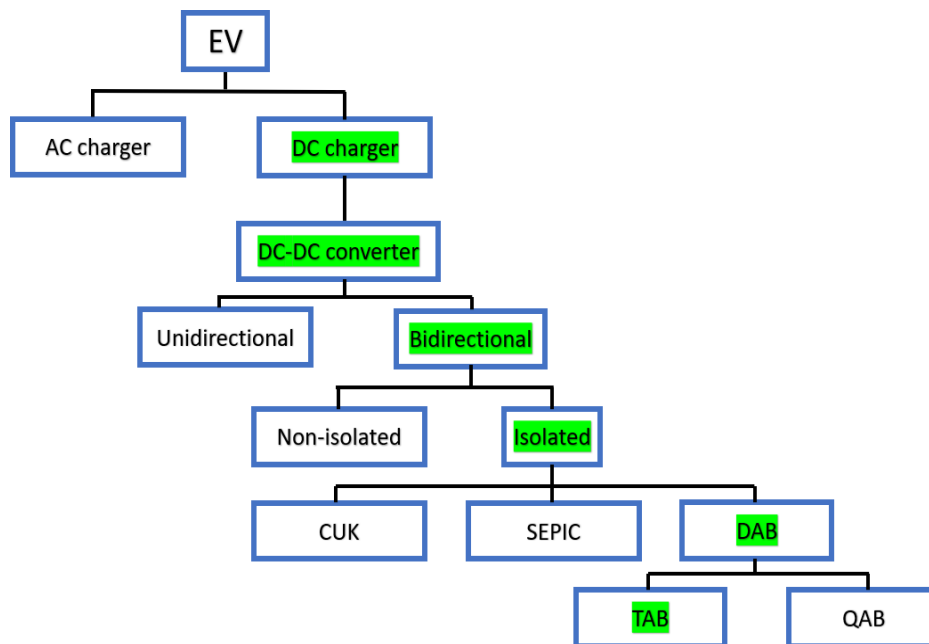


Figure 2.9 Summary of the literature for the project

CHAPTER 3

METHODOLOGY

3.1 Introduction

This chapter discussed the simulation work of DAB and TAB circuit. The 100-kW DAB system was simulated using MATLAB/Simulink. Then, the existing DAB was expanded to develop the three-port system, which is TAB system. The TAB circuit with various system and load was simulated using MATLAB/Simulink.

3.2 Flow Chart of the Project

The project starting with the objective 1 which is to design the 100 kW two-ports electric vehicle (EV) DC charger using DAB converter. The calculation parameters for the DAB converter system were set based on the required design parameters. After that, the design circuit is developed by using MATLAB/Simulink software. The DAB is designed using single-phase shift (SPS) modulation. the SPS modulation because it is simple and not complex to used due to only one angle need to be controlled.

After the DAB is successful working with SPS modulation, the system is applied to various phase shift angle where the maximum phase shift angle is 90° and the minimum phase shift angle is 0. The phase shift angle needs to be proportional to the DAB output power, to make the system function correctly. Secondly, objective 2 is to develop 100 kW three-ports EV DC charger using triple active bridge (TAB) DC-DC converter by using MATLAB/Simulink software. For the second objective, the TAB will be cascaded from the existing DAB circuit in objective 1.

The evaluation part for the TAB circuit then is proceeded in term of power balance for input and output side. Lastly, the system will be applied to the various phase-shift

angle and load systems in order to analyze the efficiency performance. Figure 3.1 shows the overview of the flow chart of this project.

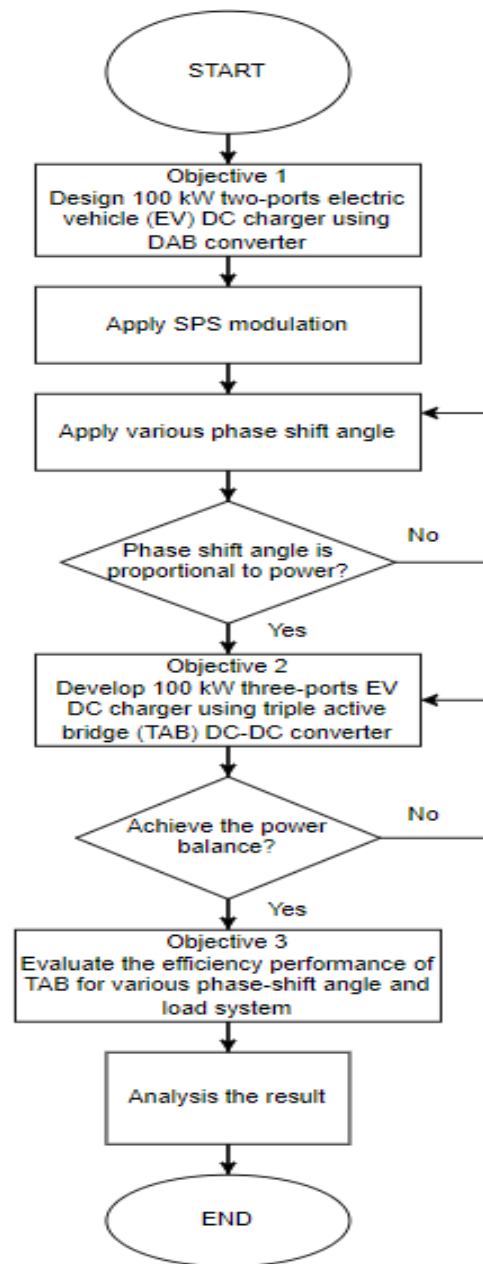


Figure 3.1 Flowchart of the project

3.3 Theoretical Calculation

3.3.1 DAB system

Table 3.1 consists of the parameters that have been used for calculation of DAB DC-DC converter. Due to the high-power application, the rated power, P_{out} that be used is 100 kW. The input voltage, V_{in} of this system is 500 V, and the output voltage, V_{out} is 850 V. Besides that, this system also uses a high switching frequency, f_{sw} which is 16 kHz.

Table 3.1 Parameters for DAB system

Description	Value
Rated Power, P_{out}	100 kW
Input Voltage, V_{in}	500 V
Output Voltage, V_{out}	850 V
Switching Frequency, f_{sw}	16 kHz
Leakage Inductor, L_k	16.60 μH
Turn Ratio, n	1:2

Several parameters such as input voltage, output voltage, switching frequency, output power and turn ratio has been taken from this paper [13] as stated in Table 3.1. From that parameter, the resistor, R and leakage inductor, L_k can be found by using the equation 3.1 where the value of L_k is equal to 16.60 μH . The maximum of phase-shift angle is used in this calculation, which is $a = 90^\circ$. The value of a need to be converted into radian by using the equation 3.2 where the θ is equal to 1.5708 rad.

$$P = \left(\frac{N \times V_{in} \times V_{out} \times \theta}{2\pi f_{sw} \times L_k} \right) \times \left(1 - \frac{\theta}{\pi} \right) \quad 3.1$$

$$100 = \left(\frac{0.5 \times 500 \times 850 \times 1.5708}{2\pi \times 16k \times L_k} \right) \times \left(1 - \frac{1.5708}{\pi} \right)$$

$$L_k = 16.60 \mu H$$

$$\theta = \left(\frac{a^\circ \times \pi}{180^\circ} \right) \quad 3.2$$

3.3.2 TAB System

Table 3.2 shows the parameter for TAB system. The main system used 100 kW, 500 V for the input voltage, 850 V for the output voltage, 16 kHz for switching frequency and turn ratio is set as 1:1:1.

Table 3.2 Parameters for TAB system

Description	Value
Rated Power, P_{out}	100 kW
Input Voltage, V_{in}	500 V
Output Voltage, V_{out}	850 V
Switching Frequency, f_{sw}	16 kHz
Leakage Inductor, L_k	10.5 μH :33 μH : 33 μH
Turn Ratio, n	1:1:1

The value of leakage inductor, L_k for the TAB have slightly different with the value L_k DAB circuit due to achieve power balance between Port 1, P1, Port 2, P2 and Port 3, P3. From the Table 3.2, current and resistor for 75 kW, 50 kW and 25 kW system can be calculated by using 3.3 and 3.4.

$$P = I \times V \quad 3.3$$

$$V = I \times R \quad 3.4$$

For 75kW system:

$$I = \left(\frac{75 \text{ k}}{850 \text{ V}} \right) = 88.24 \text{ A}$$

$$R = \left(\frac{850 \text{ V}}{88.24 \text{ A}} \right) = 9.63 \Omega$$

For 50kW system:

$$I = \left(\frac{50 \text{ k}}{850 \text{ V}} \right) = 58.82 \text{ A}$$

$$R = \left(\frac{850 \text{ V}}{58.82 \text{ A}} \right) = 14.45 \Omega$$

For 25kW system:

$$I = \left(\frac{25 \text{ k}}{850 \text{ V}} \right) = 29.41 \text{ A}$$

$$R = \left(\frac{850 \text{ V}}{29.41 \text{ A}} \right) = 28.9 \Omega$$

3.4 Simulation Design of DAB

This simulation of DAB converter circuit is designed by using MATLAB/Simulink software. This circuit is used for high power application. Table 3.1 tabulates the parameters of the simulation DAB DC-DC converter. The rated power of the circuit is expected at 100 kW with maximum phase-shift angle which is 90°. The input voltage is set at 500 V and the expected output voltage is 850 V. Due to the high-power application, switching frequency that been used in this system us 16 kHz. Based on the theoretical calculation, the value of leakage inductor that be used is 16.60 μH .

3.4.1 DAB Converter for Forward Direction

In forward direction of DAB DC-DC converter, the power flow from the primary side to secondary side. The primary side is acting as source or supply and the secondary side acts as a load. Figure 3.2 shows the forward circuit of DAB DC-DC converter. The source of the primary side can be any DC sources, while at the secondary side, it can be the load which is battery of EV. In the forward direction, the voltage pulse in primary side is leading voltage pulse in the secondary side with a certain value of phase-shift angle.

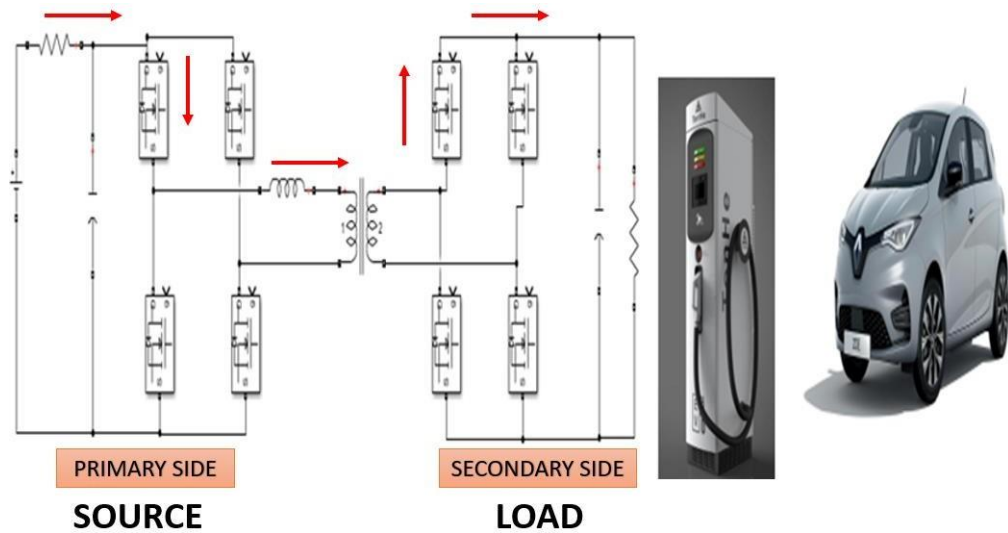


Figure 3.2 DAB converter for forward direction

3.4.2 DAB Converter for Reverse Direction

For reverse direction in DAB DC-DC converter, the power is flowing from the secondary side to the primary side through the high frequency transformer. In this mode, the secondary side acts as a source and the primary side functions as load. Figure 3.3 shows the DAB DC-DC converter for the reverse direction. In the reverse direction, the voltage pulse in primary side is lagging to the voltage pulse in secondary side with a certain value of phase-shift angle.

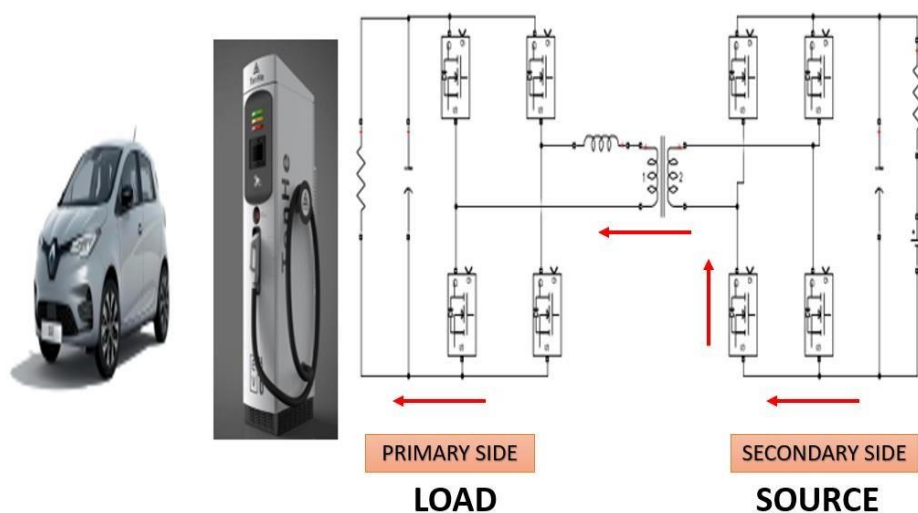


Figure 3.3 DAB converter reverse direction

Figure 3.4 shows the pulse generator in MATLAB/Simulink for set up the phase shift angle. It shows that the phase delay at the primary side have been set with 90° . The primary side will receive the maximum load from the secondary side in the reverse DAB circuit.

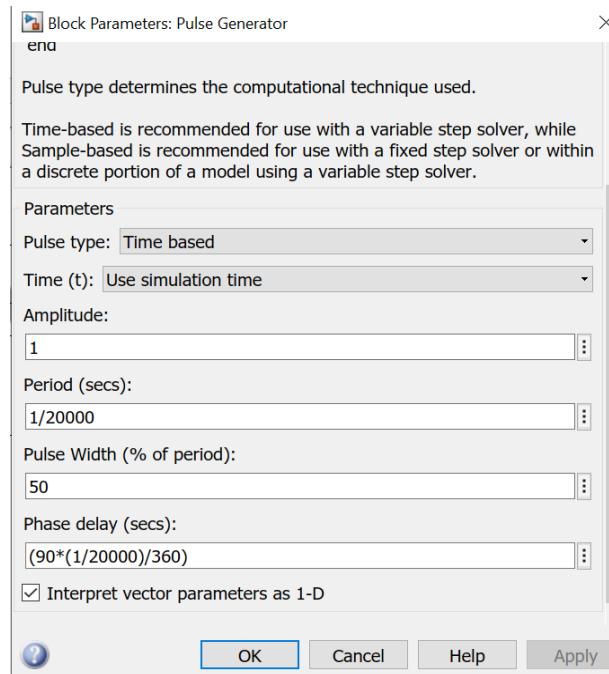


Figure 3.4 Pulse generator setting for primary side

Figure 3.5 display the pulse generator setting for the secondary side. The phase delay will be set with 0 value. It is because the secondary side function as a source. This pulse generator shows the different setting between the primary side and secondary side of the circuit.

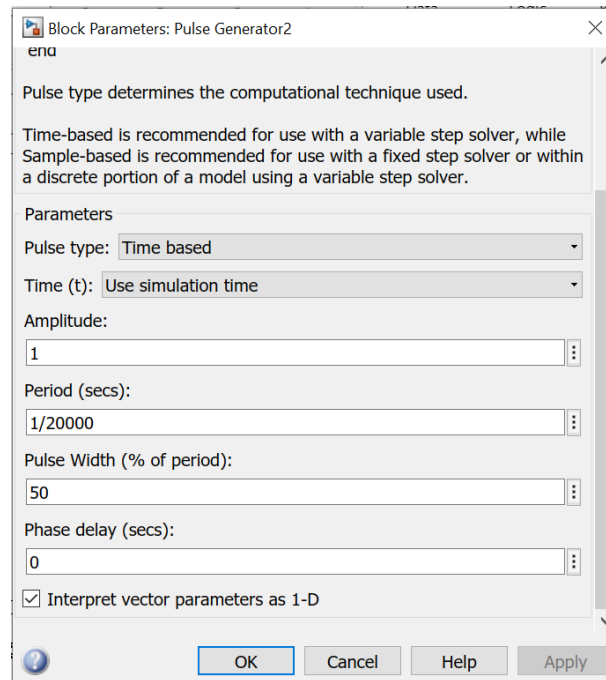


Figure 3.5 Pulse generator setting for secondary side

3.5 Simulation Design of TAB

This simulation of TAB converter circuit is design by using MATLAB/Simulink software. This circuit is design for high power application. The Table 3.3 shows the parameters of the simulation TAB DC-DC converter. The rated power of the circuit is expected at 100 kW with maximum phase-shift angle which is 90° . The input voltage is set at 500 V and the expected output voltage is 850 V. Due to the high-power application, switching frequency that been used in this system us 16 kHz.

3.5.1 TAB Converter

TAB can be developed with flexible design of input and output. It can be developed or design with one-input-source-two-output-load or two-input-source-one-output-load. If it designs with configuration one-source-two-load, one of the ports will be the source and the other two port will be as load as shown in Figure 3.6. If it designs with two-input-source-one-output-load, two ports will be connected to the grid or renewable energy source and one port will be the load as show in Figure 3.7. The suitable design of structure is determined based on the input and output data.

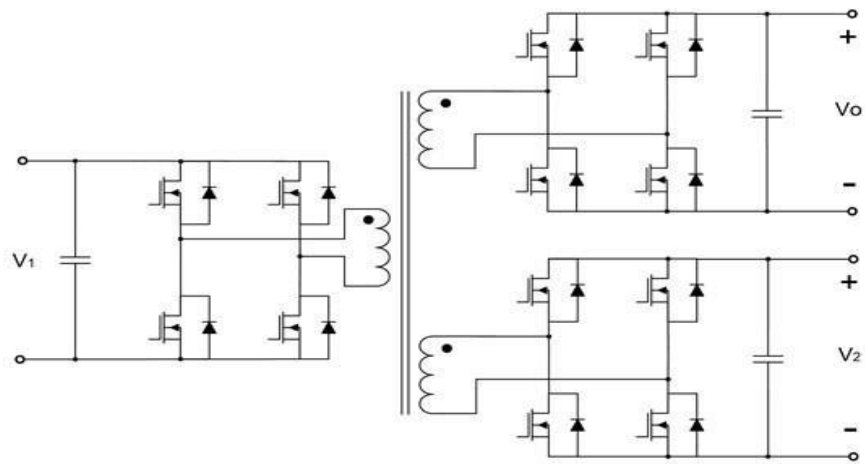


Figure 3.6 One-input-two-output configuration

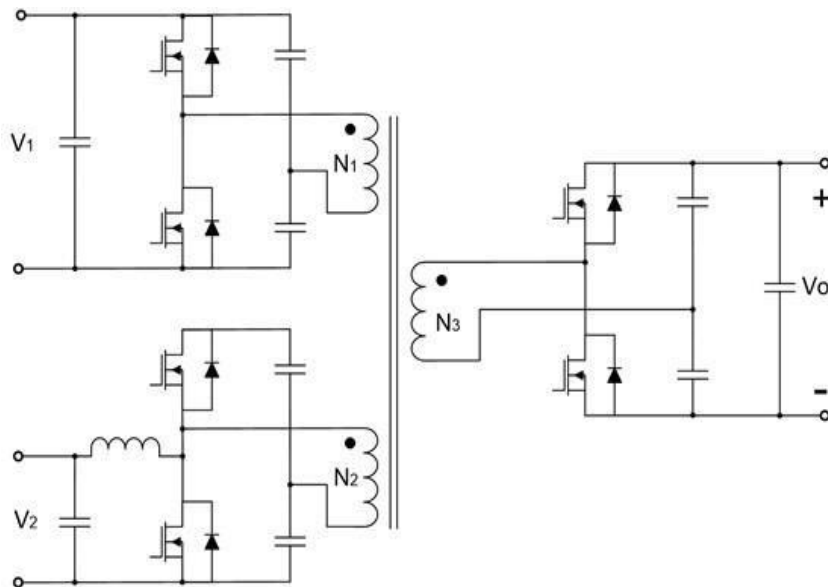


Figure 3.7 Two-input-one-output configuration

High efficiency is a desirable characteristic for this converter. The power-flow can be bidirectional because both bridges are operational. The two converters' power switches work at the same frequency switching, but with different duty cycles. The phase shifts control the power flow between the three ports. The power flow is going through the multi-winding transformer. The transformer is an important part of the system. The transformer is used to transfer power, and inductors are used as energy transfer elements. It offers voltage matching and isolation.

When the switching frequency is fixed, phase shifts and leakage inductances affect the power flow through the transformer [35]. While transmitting the same amount of power, a smaller leakage inductance leads to a smaller phase shift. The transformer's leakage inductance is key since it is responsible for power transmission. Figure 3.6 show the TAB converter circuit.

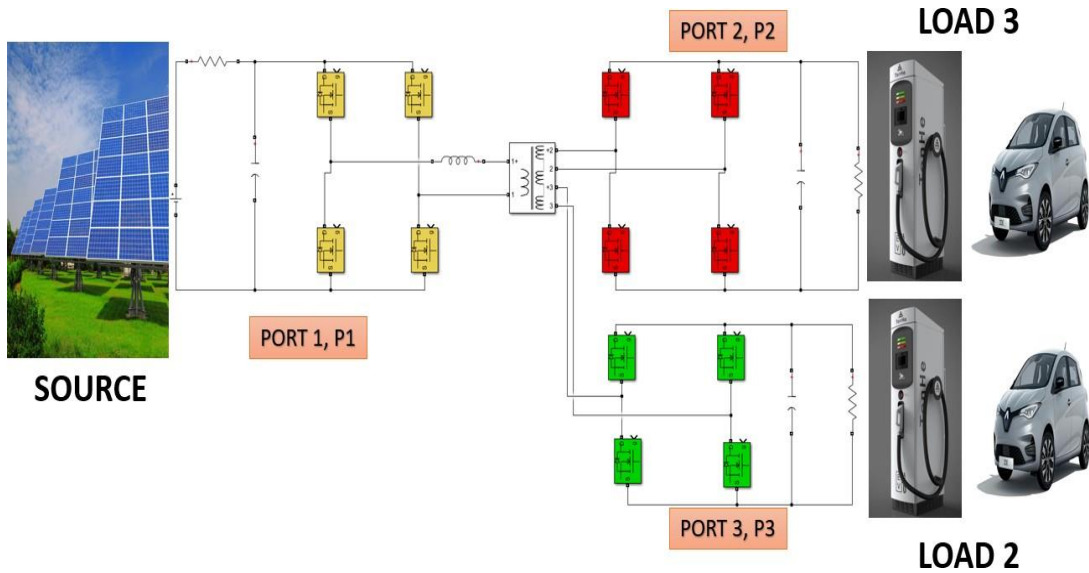


Figure 3.8 TAB converter circuit

CHAPTER 4

RESULTS AND DISCUSSION

4.1 Introduction

This chapter summarised the results of the DAB circuit using 100 kW system models that are constructed by using MATLAB/Simulink. The performance of the DAB system has been analyzed in forward direction and reverse direction. Besides, the results of TAB circuit with various load systems also have been explained in details. The efficiency of the TAB system has been evaluated for various phase-shift angle and loads.

4.2 Simulation Results for Dual Active Bridge System

4.2.1 Results for DAB in Forward Direction

Figure 4.1 shows the result of the voltage pulse of the primary side and secondary side for the forward direction DAB DC-DC converter with the maximum phase angle of 90° . The voltage pulse of primary side, V1 is leading the voltage pulse of secondary side, V2 or the secondary side, V2 is lagging the primary side, V1 by 90° . The shifting between the both pulses changed according to the value of phase-shift angle that was setting in pulse generator. The value of voltage in the primary side is 200 V while for the value of voltage in the secondary side is 400 V.

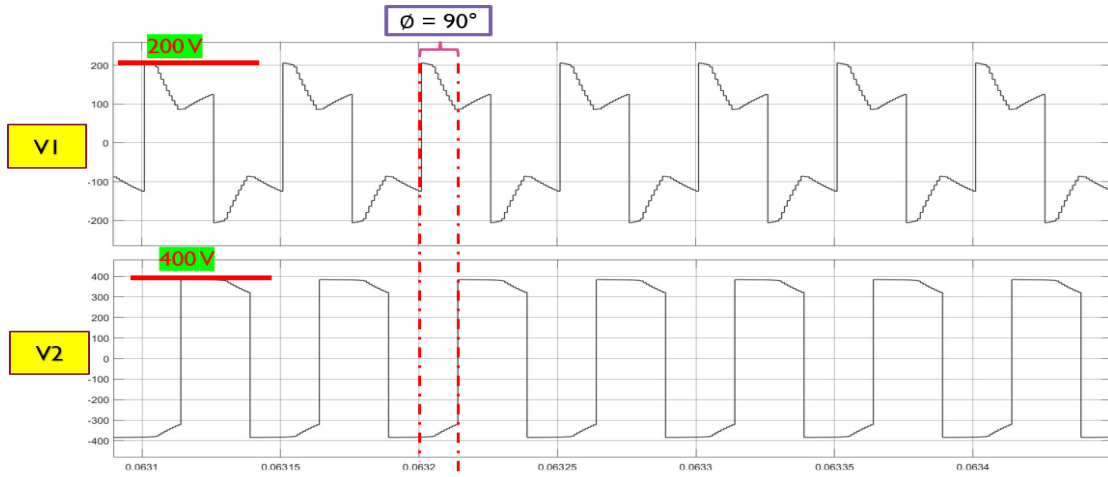


Figure 4.1 Voltage pulse at primary and secondary side in forward direction

In the forward direction, the converter's output voltage and output current are shown in the Figure 4.2 at 90° of phase-shift angle. The output voltage for the DAB DC-DC converter in forward direction with 90° phase-shift angle is 380 V. Due to the losses, the value of output voltage is slightly drop. The output current for the forward circuit with the maximum phase-shift angle is 71 A.

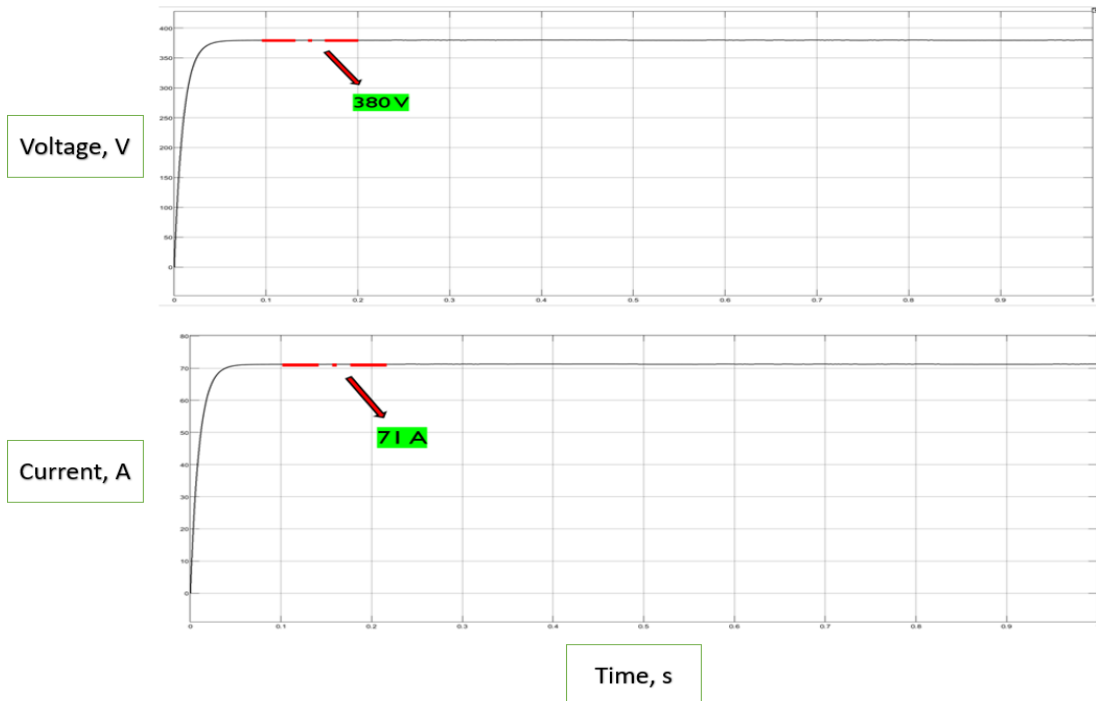


Figure 4.2 Output volatge and output current for forward circuit at 90°

4.2.2 Results for DAB in Reverse Direction

Reverse direction is the power flow from the secondary side to primary side. The secondary side will act as source or supply and the primary side will act as load. Figure 4.3 displays the results of the voltage pulse waveform of the transformer in reverse direction of DAB DC-DC converter circuit with maximum phase angle 90° . The value of voltage in primary side is 200 V and the secondary side is 400 V. The reverse direction of DAB DC-DC converter can be analyzed. It shows the voltage pulse of primary side, V1 is lagging with the voltage pulse at secondary side, V2 or the secondary side, V2 is leading the primary side, V1 by 90° .

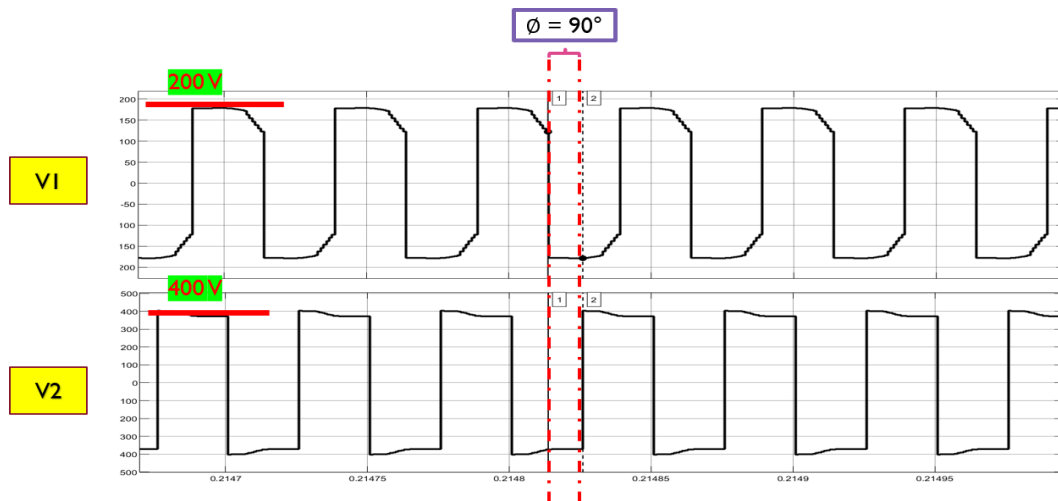


Figure 4.3 Primary and secondary voltage

Figure 4.4 demonstrates the output voltage and output current for the reverse direction of the DAB DC-DC converter at 90° of phase-shift angle. The value of the output voltage of the DAB DC-DC converter in reverse direction is 173 V as shown in Figure 4.4. The value of the output voltage is different with the input voltage due to the losses in the circuit. The value of the output current is 130 A with the maximum phase-shift angle which is 90° .

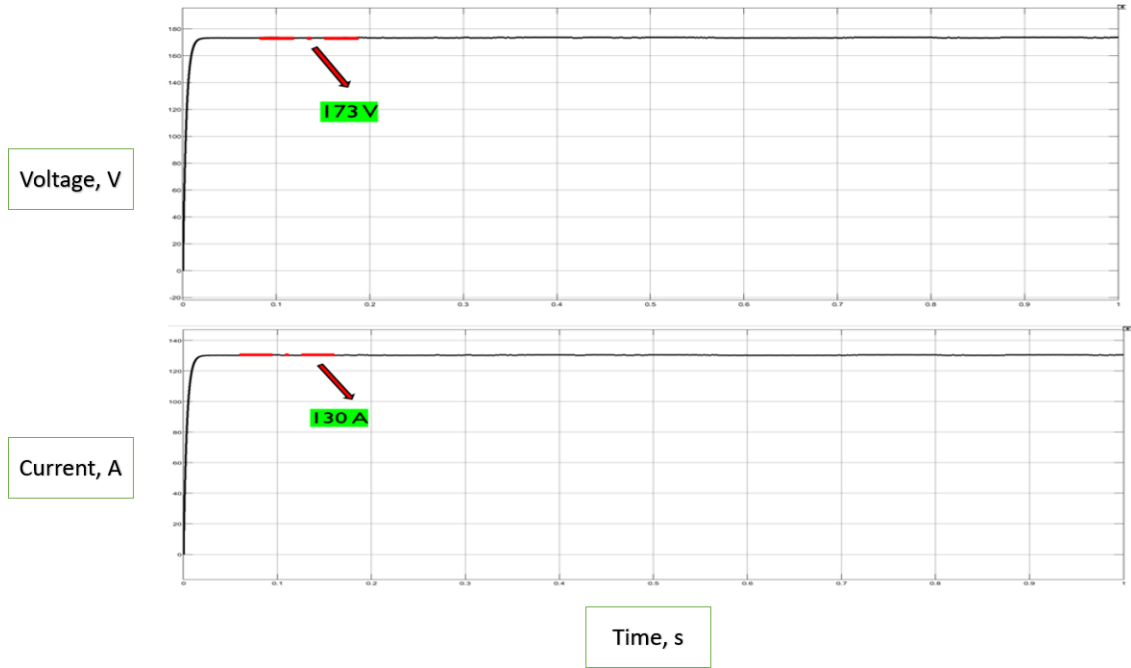


Figure 4.4 Output voltage and output current for reverse direction

4.3 Simulation Results for Triple Active Bridge System

4.3.1 100 kW TAB System

The table 4.1 illustrates the result simulation of the 100-kW system for TAB. It shows that the input power, output power port 2, output current port 2, output voltage port 2, output power port 3, output current port 3, output voltage port 3 and efficiency for same phase shift angle at load sides.

Table 4.1 Result of the 100 kW TAB system (same phase-shift angle at the output side)

ϕ (°)	Pin (kW)	Po P2 (kW)	Io P2 (A)	Vo P2 (V)	Po P3 (kW)	Io P3 (A)	Vo P3 (V)	η (%)
0 : 90 : 90	106	53	114	465	53	114	465	100
0 : 75 : 75	94	46	100	466	46	100	466	97
0 : 60 : 60	75	34	79	438	34	79	438	93
0 : 45 : 45	58	23	61	386	23	61	386	81
0 : 25 : 25	47	12	48	265	12	48	265	55

From the table 4.1, when both port 2 and port 3 is set to 90° which is the maximum phase shift angle, the efficiency is 100%. Besides that, the value of output voltage and current for port 2 is equal to output voltage and current in port 3 and it shows the power

balance between the input and output side. When the port 2 and port 3 is set to 25° angle for, the efficiency is 55% which is lowest efficiency for this system. From the results it shows that the efficiency is decrease when the phase-shift angle decreases and the higher efficiency occurs at the maximum phase shift angle.

Figure 4.5 shows the output waveform for all ports when both secondary side of 100kW TAB is applied with 90° . The input voltage value for port 1 is 466 V and the input current for port 1 is 228 A. While for output side, the value of the output voltage and output current for port 2 and port 3 is same which is 465 V and 114 A, respectively.

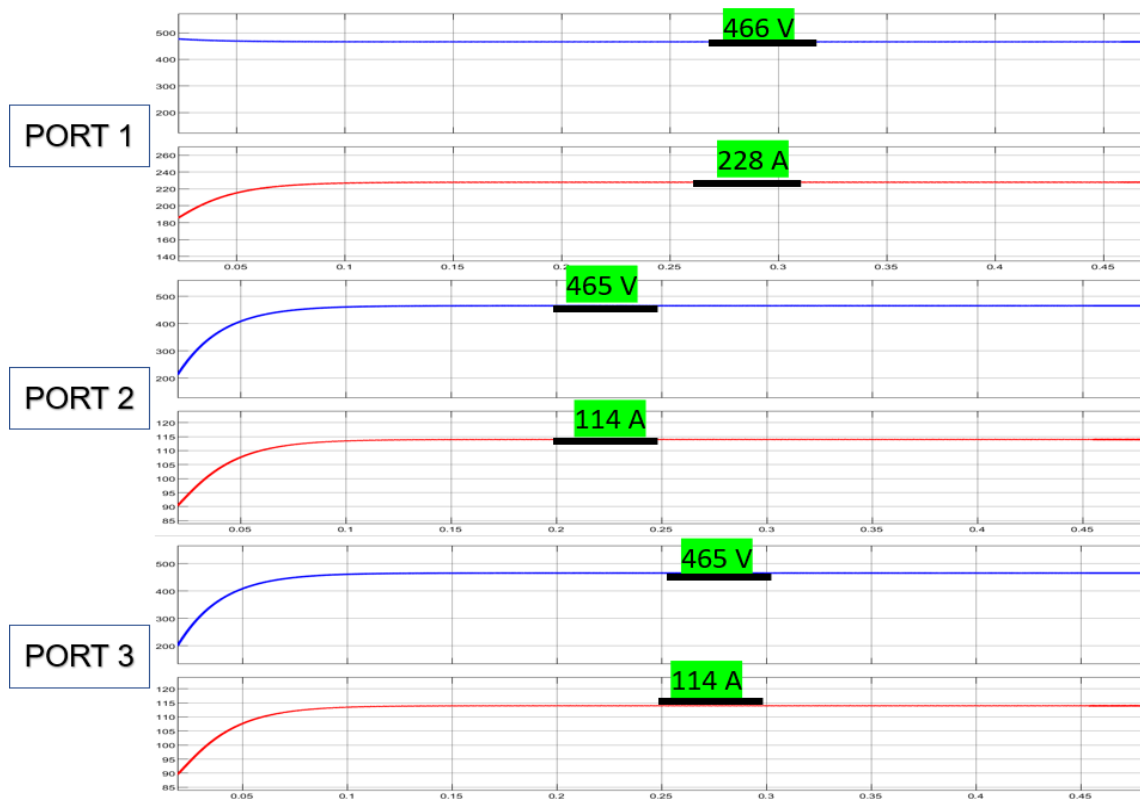


Figure 4.5 Output voltage and current for 100kW with $0^\circ:90^\circ:90^\circ$

Table 4.2 shows the result for 100 kW TAB system when the load sides were applied with different phase-shift angle, where the port 2 have been set fixed at 90° angle and port 3 with various phase-shift angle.

Table 4.2 Result of the 100 kW TAB system (different phase-shift angle at the output side)

ϕ (°)	Pin (kW)	Po P2 (kW)	Io P2 (A)	Vo P2 (V)	PoP3 (kW)	Io P3 (A)	Vo P3 (V)
0 : 90 : 75	101	62	124	508	37	88	419
0 : 90 : 60	104	40	76	526	28	83	341
0 : 90 : 45	99	50	94	531	15	58	258
0 : 90 : 25	103	53	105	508	6.9	60	116
0 : 90 : 0	111	49	103	476	6.5	88	7.4

With the different phase shift angle apply at the port 3, it shows the different value of output between these two ports. From the table, it shows the output power for port 2 is higher than the port 3 due to port 2 have the higher phase-shift angle which is 90°. The output voltage and output current also have a different value due to the different phase shift angle. However, the total of output power for port 2 and port 3 are equal to the output power of port 1. Hence, it shows that the power in TAB are still balance even the phase-shift angles are different at port 2 and port 3.

Figure 4.6 shows the output waveform for all ports when secondary side of 100kW TAB is applied with 90° and 45° at port 2 and port 3, respectively. The input voltage and current value for this condition is 473 V and 180 A. From the Figure 4.2, the output voltage for port 2 is higher than port 3 which is 525 V for port 2 and 258 V for port 3. The output current for port 2 is also greater than the output current for port 3, measuring 152 A versus 58.9 A.

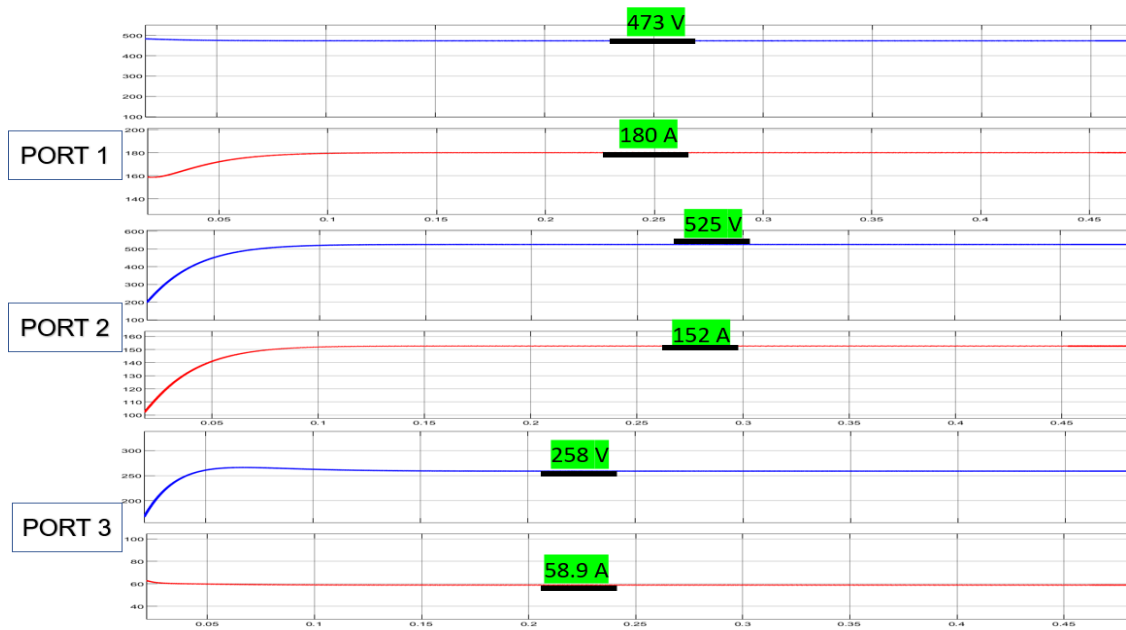


Figure 4.6 Output voltage and current for 100kW with 0°:90°:45°

4.3.2 75 kW TAB System

The table 4.3 illustrates the result simulation of the 75-kW system for TAB. It shows that the input power, output power port 2, output current port 2, output voltage port 2, output power port 3, output current port 3, output voltage port 3 and efficiency for same phase shift angle at load sides.

Table 4.3 Result of the 75 kW TAB system (same phase shift angle at the output side)

ϕ (°)	P_{in} (kW)	$P_o P2$ (kW)	$I_o P2$ (A)	$V_o P2$ (V)	$P_o P3$ (kW)	$I_o P3$ (A)	$V_o P3$ (V)	η (%)
0 : 40 : 40	54	26	63	465	26	59	464	97
0 : 30 : 30	46	18	52	385	18	47	385	80
0 : 25 : 25	40	14	71	348	14	41	347	70
0 : 15 : 15	48	11	70	239	11	49	237	48
0 : 10 : 10	56	9.6	83	171	9.6	57	167	34

From the table 4.3, when both port 2 and port 3 is set to 40° which is the maximum phase shift angle, the efficiency is 97%. Besides that, the value of output voltage and current for port 2 is equal to output voltage and current in port 3 and it shows the power balance between the input side and output side. When the port 2 and port 3 is set to 10° angle for the efficiency is 34% which is lowest efficiency for this system. From the result

it shows that the efficiency is decrease when the phase shift angle decreases and the higher efficiency occurs at the maximum phase shift angle.

Figure 4.7 shows the output waveform for all ports when both secondary side of the 75kW TAB is applied with 40°. The input voltage value for port 1 is 479 V and the input current for port 1 is 113 A. While for output side, the value of the output voltage and output current for port 2 and port 3 is same which is 464 V and 56 A, respectively.

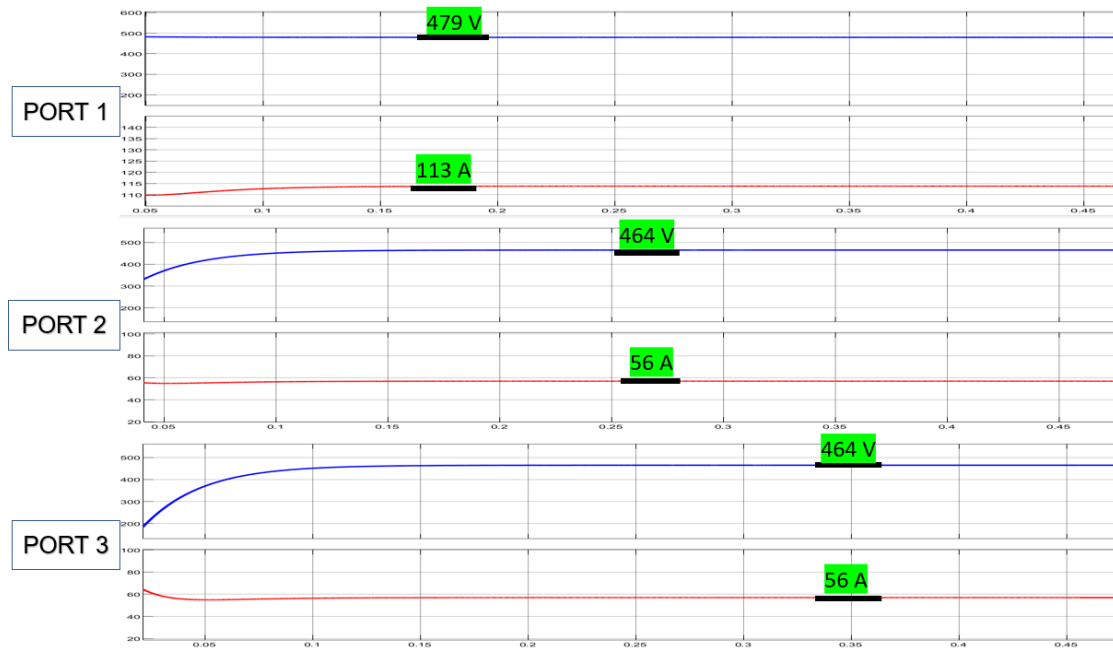


Figure 4.7 Output voltage and current for 75kW with 0°:40°:40°

Table 4.4 shows the result for 75 kW TAB system when the load sides were applied with different phase-shift angle, where the port 2 have been set fixed at 40° angle and port 3 with various phase-shift angle.

Table 4.4 Result of the 75 kW TAB system (different phase-shift angle at the output side)

ϕ (°)	Pin (kW)	Po P2 (kW)	Io P2 (A)	Vo P2 (V)	PoP3 (kW)	Io P3 (A)	Vo P3 (V)
0 : 40 : 30	48	41	84	488	26	80	335
0 : 40 : 25	47	34	69	499	14	50	282
0 : 40 : 15	49	37	77	493	11	80	139
0 : 40 : 10	53	36	74	481	5	93	57
0 : 40 : 0	57	34	74	470	1	104	1

With different phase-shift angle apply at the port 3, it shows the different value of output between these two ports. From the table, it shows the output power for port 2 is higher than the port 3 due to port 2 have the higher phase-shift angle which is 40° . The output voltage and output current also have a different value due to the different phase-shift angle. However, the total of output power for port 2 and port 3 are equal to the output power of port 1. Hence, it shows that the power in TAB are still balance even the phase-shift angles are different at port 2 and port 3.

Figure 4.8 shows the output waveform for all ports when secondary side of 75kW TAB is applied with 40° and 10° at port 2 and port 3, respectively. The input voltage and current value for this condition is 485 V and 110 A. From the Figure 4.8, the output voltage for port 2 is higher than port 3 which is 481 V for port 2 and 57 V for port 3.

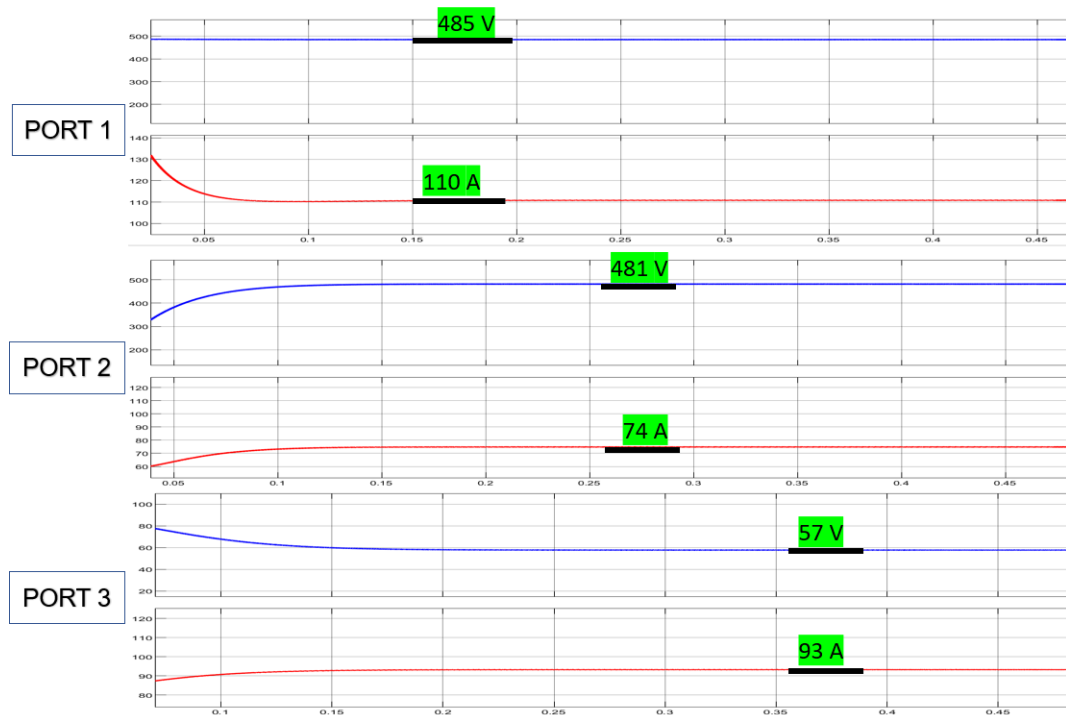


Figure 4.8 Output voltage and current for 75kW with $0^\circ:40^\circ:10^\circ$

4.3.3 50 kW TAB System

The table 4.5 illustrates the result simulation of the 50-kW system for TAB. It shows that the input power, output power port 2, output current port 2, output voltage port 2, output power port 3, output current port 3, output voltage port 3 and efficiency for same phase shift angle at load sides.

Table 4.5 Result of the 50 kW TAB system (same phase-shift angle at the output side)

ϕ (°)	Pin (kW)	Po P2 (kW)	Io P2 (A)	Vo P2 (V)	PoP3 (kW)	Io P3 (A)	Vo P3 (V)	η (%)
0 : 25 : 25	38	19	39	495	19	39	495	99
0 : 24 : 24	39	19	41	474	19	41	474	98
0 : 20 : 20	31	13	31	415	13	31	415	85
0 : 15 : 15	37	12	37	344	12	37	344	70
0 : 10 : 10	45	11	46	244	11	46	244	48

From the table 4.5, when both port 2 and port 3 is set to 25° which is the maximum phase shift angle, the efficiency is 99%. Besides that, the value of output voltage and current for port 2 is equal to output voltage and current in port 3 and it shows the power balance between the input and output side. When the port 2 and port 3 is set to 10° angle for the efficiency is 48% which is lowest efficiency for this system. From the results it shows that the efficiency is decrease when the phase-shift angle decreases and the higher efficiency occurs at the maximum phase-shift angle.

Figure 4.9 shows the output waveform for all ports when both secondary side of 50kW TAB is applied with 25°. The input voltage value for port 1 is 485 V and the input current for port 1 is 78 A. While for the output side, the value of the output voltage and output current for port 2 and port 3 is same which is 495 V and 39 A, respectively.

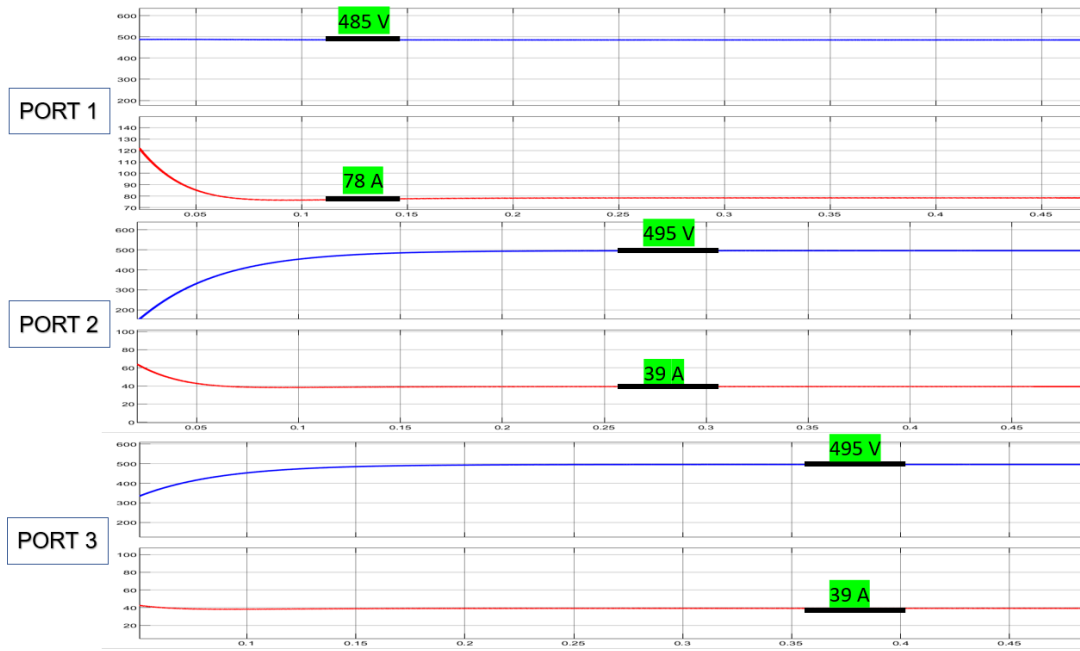


Figure 4.9 Output voltage and current for 50 kW with 0°:25°:25°

Table 4.6 shows the result for 50 kW TAB system when the load sides were applied with different phase-shift angle, where the port 2 have been set fixed at 25° angle and port 3 with various phase-shift angle.

Table 4.6 Result of the 50 kW TAB system (different phase-shift angle at the output side)

ϕ (°)	Pin (kW)	Po P2 (kW)	Io P2 (A)	Vo P2 (V)	PoP3 (kW)	Io P3 (A)	Vo P3 (V)
0 : 25 : 8	39	30	58	527	9	84	116
0 : 25 : 7	42	31	60	519	7	94	79
0 : 25 : 6	42	31	60	519	7	94	79
0 : 25 : 5	44	30	58	514	5	97	52
0 : 25 : 0	47	30	58	505	1	108	13

With the different phase shift angle apply at the port 3, it shows the different value of output between these two ports. From the table, it shows the output power for port 2 is higher than the port 3 due to port 2 have the higher phase-shift angle which is 25°. The output voltage and output current also have a different value due to the different phase shift angle. However, the total of output power for port 2 and port 3 are equal to the output power of port 1. Hence, it shows that the power in TAB are still balance even the phase-shift angles are different at port 2 and port 3.

Figure 4.10 shows the output waveform for all ports when secondary side of 50kW TAB is applied with 25° and 5° at port 2 and port 3, respectively. The input voltage and current value for this condition is 488 V and 90 A. From the Figure 4.10, the output voltage for port 2 is higher than port 3 which is 514 V for port 2 and 52 V for port 3.

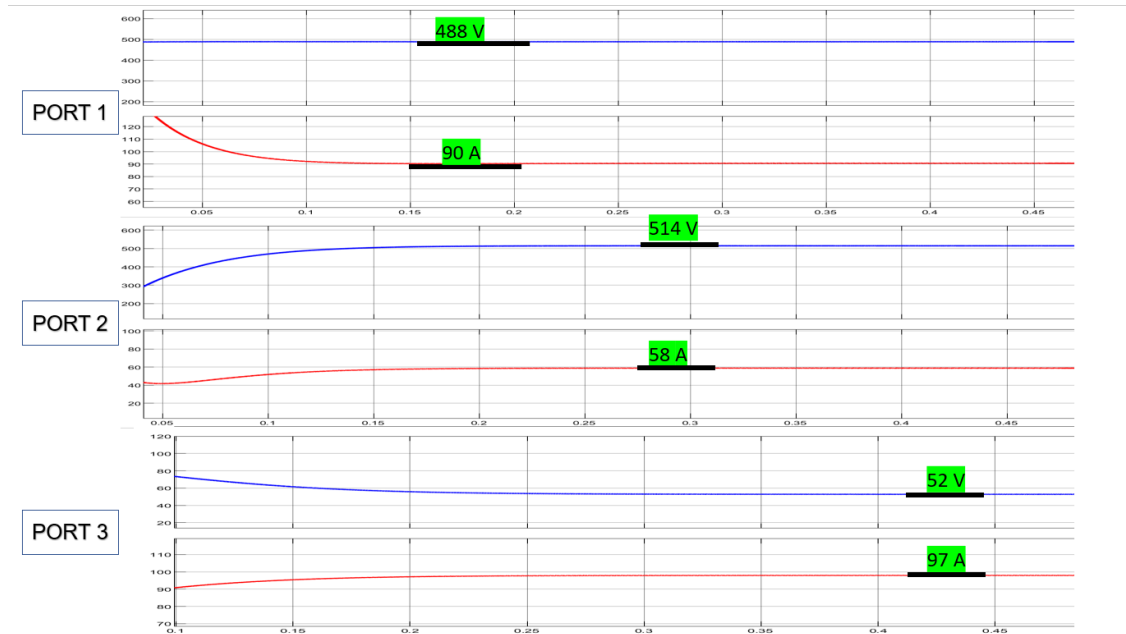


Figure 4.10 Output voltage and current for 50kW with 0°:25°:5°

4.3.4 25 kW TAB System

The table 4.7 illustrates the result simulation of the 25-kW system for TAB. It shows that the input power, output power port 2, output current port 2, output voltage port 2, output power port 3, output current port 3, output voltage port 3 and efficiency for same phase shift angle at load sides.

Table 4.7 Result of the 25 kW TAB system (same phase-shift angle at the output side)

ϕ (°)	Pin (kW)	Po P2 (kW)	Io P2 (A)	Vo P2 (V)	PoP3 (kW)	Io P3 (A)	Vo P3 (V)	η (%)
0 : 11 : 11	17	8	19	487	8	17	487	94
0 : 10 : 10	26	11.7	16	438	11.7	26	438	90
0 : 9 : 9	26	11	16	438	11	26	438	85
0 : 8 : 8	20	8.4	42	401	8.4	21	400	84
0 : 5 : 5	32	10	55	307	10	33	304	62

From the table 4.7, when both port 2 and port 3 is set to 11° which is the maximum phase shift angle, the efficiency is 94%. Besides that, the value of output voltage and current for port 2 is equal to output voltage and current in port 3 and it shows the power balance between the input and output side. When the port 2 and port 3 is set to 5° angle for, the efficiency is 62% which is lowest efficiency for this system. From the results it shows that the efficiency is decrease when the phase-shift angle decreases and the higher efficiency occurs at the maximum phase shift angle.

Figure 4.11 shows the output waveform for all ports when both secondary side of 25kW TAB is applied with 11° . The input voltage value for port 1 is 492 V and the input current for port 1 is 35 A. While for output side, the value of the output voltage and output current for port 2 and port 3 is same which is 487 V and 19 A, respectively.

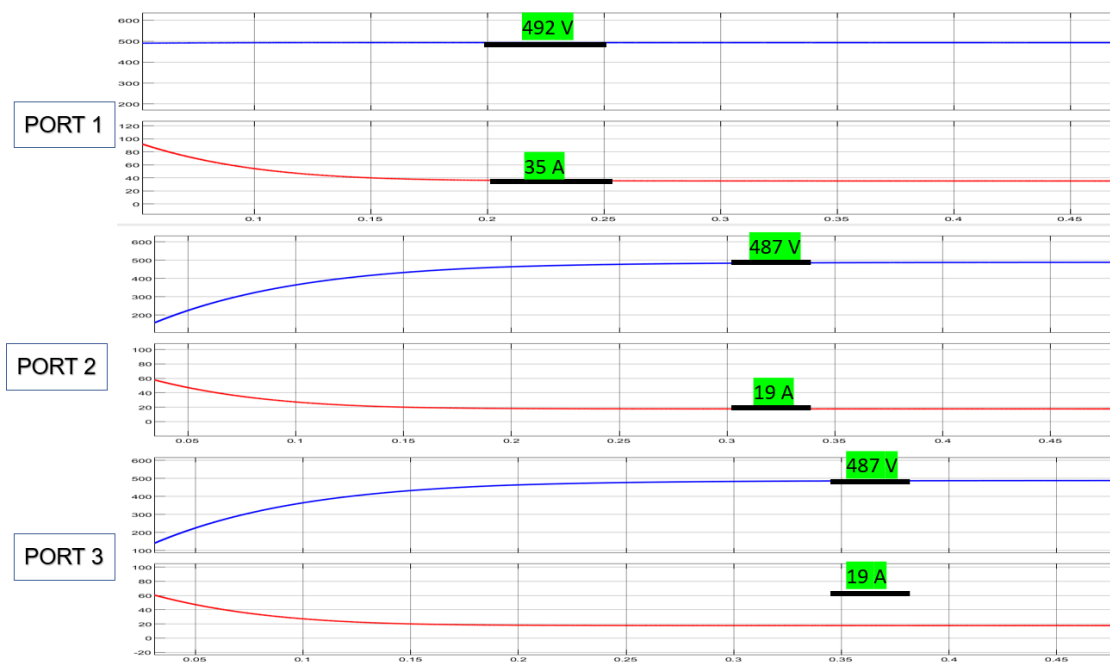


Figure 4.11 Output voltage and current for 25kW with $0^\circ:11^\circ:11^\circ$

Table 4.8 shows the result for 25 kW TAB system when the load sides were applied with different phase-shift angle, where the port 2 have been set fixed at 11° angle and port 3 with various phase-shift angle.

Table 4.8 Result of the 25 kW TAB system (different phase-shift angle at the output side)

ϕ (°)	Pin (kW)	Po P2 (kW)	Io P2 (A)	Vo P2 (V)	PoP3 (kW)	Io P3 (A)	Vo P3 (V)
0 : 11 : 4	28	20	39	518	13	81	164
0 : 11 : 3	28	20	39	518	13	81	164
0 : 11 : 2	32	19	36	517	9	87	111
0 : 11 : 1	38	19	38	505	4	102	42
0 : 11 : 0	41	19	38	499	1	108	15

With the different phase shift angle apply at the port 3, it shows the different value of output between these two ports. From the table, it shows the output power for port 2 is higher than the port 3 due to port 2 have the higher phase-shift angle which is 11° . The output voltage and output current also have a different value due to the different phase shift angle. However, the total of output power for port 2 and port 3 are equal to the output power of port 1. Hence, it shows that the power in TAB are still balance even the phase-shift angles are different at port 2 and port 3.

Figure 4.12 shows the output waveform for all ports when secondary side of 25kW TAB is applied with 11° and 2° at port 2 and port 3, respectively. The input voltage and current value for this condition is 492 V and 66 A. From the Figure 4.12, the output voltage for port 2 is higher than port 3 which is 517 V for port 2 and 111 V for port 3.

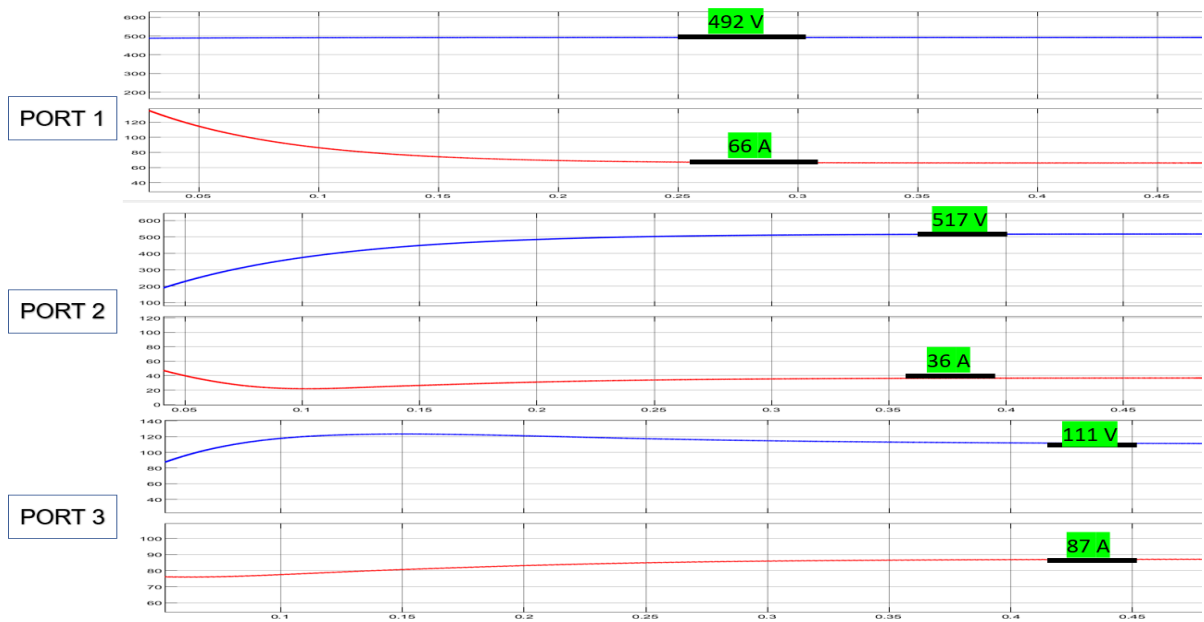


Figure 4.12 Output voltage and current for 25kW with $0^\circ:11^\circ:2^\circ$

4.4 Efficiency of the system

4.4.1 100 kW TAB System

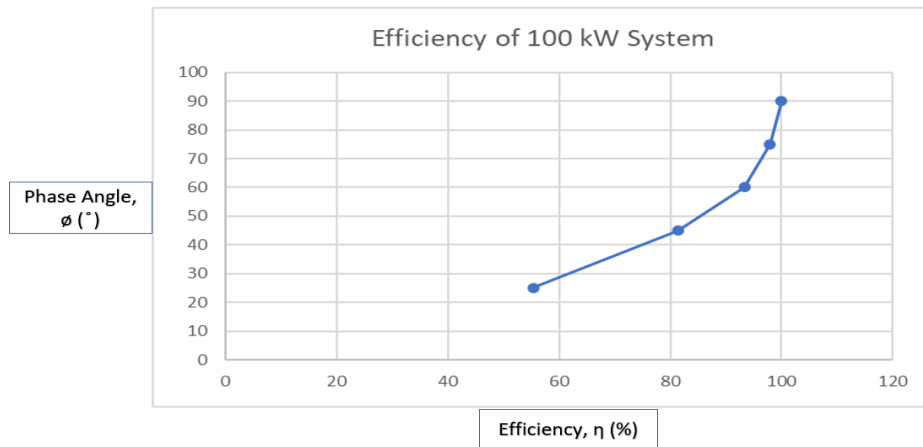


Figure 4.13 Efficiency of 100 kW TAB system

Figure 4.13 shows the graph of efficiency for the 100-kW system. It shows that the value of efficiency is increase when the higher phase shift angle is set. It reaches 100% efficiency when the maximum phase shift angle is set. The lowest efficiency is 55% occurs at 25° angle.

4.4.2 75 kW TAB System

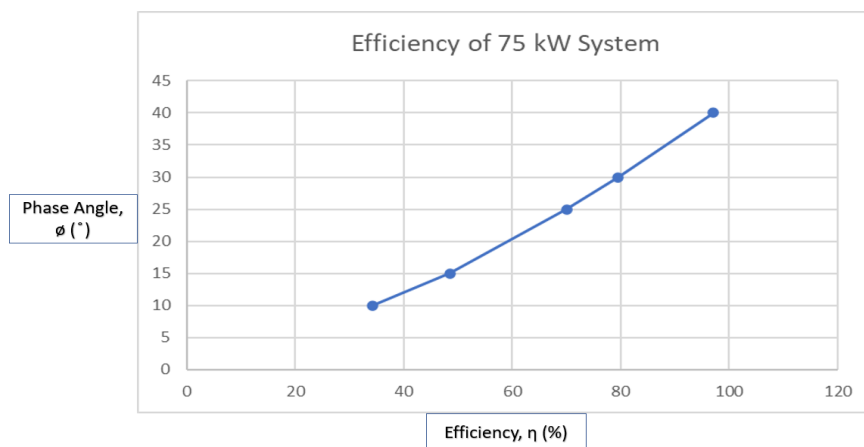


Figure 4.14 Efficiency of 75 kW TAB system

The highest efficiency occurs at 40° angle which is almost 97% that be show in the Figure 4.14. From the Figure 4.14, the lowest efficiency is 34% occurs at 10° angle. It shows that the minimum phase shift angle will equal to lower efficiency.

4.5 Discussion

From the result it can be conclude that, the DAB has more advantages which is bidirectional power flow. In the simulation, it shows that the DAB can be developed in two condition which is forward power flow and reverse power flow. Another advantage of DAB is easy to cascade. From the basic DAB circuit, TAB is easily to develop.

In the simulation, the TAB circuit has achieved the power balance between input port and output port. In TAB also, when the maximum phase shift angle is set, the efficiency value is reach almost 100%. Then, the lowest efficiency at the lowest phase shift angle. TAB also produces the output balance for all system. Lastly, it can work at various phase shift angle.

CHAPTER 5

CONCLUSION

5.1 Conclusion

In the conclusion, the two-ports electric vehicle (EV) DC charger using bidirectional dual active bridge (DAB) DC-DC converter have been designed using MATLAB/Simulink. The DAB circuit has able to reached the maximum power flow for the 100-kW system. After that, the three-ports EV DC charger using triple active bridge (TAB) DC-DC converter have been successful developed using MATLAB/Simulink. The power balance has been achieved between the output port 2 and output port 3. Lastly, the efficiency performance of TAB for various phase-shift angle and load system have been analysed. It has been showed that the 100-kW system is have the greatest efficiency among with the various system and load by producing average 86%. The higher efficiency occurs at the maximum phase shift angle by producing 100% and the lowest efficiency occurs at the lowest phase shift angle with 55%.

5.2 Recommendation

In this research, the high efficiency isolated three-port DC-DC converter for DC charger stations has been developed. With the advantages of the DAB circuit, it easily cascades into TAB and has been designed. It has been tested with the 100kW, 75kW, 50kW and 25kW system to study the efficiency. Other than that, the efficiency between various load system has been evaluate. The 100kW system have show the better efficiency compare to other system.

More research could be conducted for further study which is how to decrease the power loss for the high system of the DC-DC converter. Other than that, to designed the multiport converter that have more than three-port and evaluate its efficiency.

REFERENCES

- [1] “• Malaysia: car ownership among consumers by type 2019 | Statista.” <https://www.statista.com/statistics/1029295/malaysia-car-ownership-among-consumers-by-type/> (accessed Jan. 14, 2022).
- [2] “Sources of Greenhouse Gas Emissions | US EPA.” <https://www.epa.gov/ghgemissions/sources-greenhouse-gas-emissions> (accessed Jan. 14, 2022).
- [3] M. Steinheimer, U. Trick, and P. Ruhrig, “Energy communities in Smart Markets for optimisation of peer-to-peer interconnected Smart Homes,” *Proc. 2012 8th Int. Symp. Commun. Syst. Networks Digit. Signal Process. CSNDSP 2012*, 2012, doi: 10.1109/CSNDSP.2012.6292732.
- [4] “Green Tech Definition.” https://www.investopedia.com/terms/g/green_tech.asp (accessed Jan. 14, 2022).
- [5] “Electric Car Statistics and Facts 2021 | Policy Advice.” <https://policyadvice.net/insurance/insights/electric-car-statistics/> (accessed Jan. 14, 2022).
- [6] “Vehicle to Grid: electric cars as localized power station. – Robotics And Machine ANalytics Laboratory.” <https://ramanlab.wordpress.com/2018/02/05/vehicle-to-grid-electric-cars-as-localized-power-station/> (accessed Jan. 16, 2022).
- [7] Y. Du, S. Lukic, B. Jacobson, and A. Huang, “Review of high power isolated bi-directional DC-DC converters for PHEV/EV DC charging infrastructure,” *IEEE Energy Convers. Congr. Expo. Energy Convers. Innov. a Clean Energy Futur. ECCE 2011, Proc.*, pp. 553–560, 2011, doi: 10.1109/ECCE.2011.6063818.
- [8] S. Inoue and H. Akagi, “A Bidirectional DC – DC Converter for an Energy,” *IEEE Trans. Power Electron.*, vol. 22, no. 6, pp. 2299–2306, 2007.
- [9] V. Monteiro, J. C. Ferreira, A. A. N. Melendez, J. A. Afonso, C. Couto, and J. L. Afonso, “Experimental Validation of a Bidirectional Three-Level dc-dc Converter for On-Board or Off-Board EV Battery Chargers,” *IECON Proc. (Industrial Electron. Conf.)*, vol. 2019-October, no. i, pp. 3468–3473, 2019, doi: 10.1109/IECON.2019.8927763.
- [10] F. Krismer, J. Biela, and J. W. Kolar, “A comparative evaluation of isolated bi-directional DC/DC converters with wide input and output voltage range,” *Conf. Rec. - IAS Annu. Meet. (IEEE Ind. Appl. Soc.)*, vol. 1, no. c, pp. 599–606, 2005, doi: 10.1109/IAS.2005.1518368.

- [11] V. Jeyakarthykha and K. R. Vairamani, "Multiport bidirectional dc-dc converter for energy storage applications," *2014 Int. Conf. Circuits, Power Comput. Technol. ICCPCT 2014*, pp. 411–417, 2014, doi: 10.1109/ICCPCT.2014.7054897.
- [12] H. P. System, B. Zhao, S. Member, Q. Song, W. Liu, and Y. Sun, "Overview of Dual-Active-Bridge Isolated Bidirectional DC – DC Converter for," vol. 29, no. 8, pp. 4091–4106, 2014.
- [13] S. Chakraborty, H. N. Vu, M. M. Hasan, D. D. Tran, M. El Baghdadi, and O. Hegazy, "DC-DC converter topologies for electric vehicles, plug-in hybrid electric vehicles and fast charging stations: State of the art and future trends," *Energies*, vol. 12, no. 8, 2019, doi: 10.3390/en12081569.
- [14] R. Kashyap and S. Rastogi, "The Need and Urgency of Electric Vehicles or EVs in World today," *Rev. Int. J. Multidiscip.*, vol. 6, no. 3, pp. 6–11, 2021, doi: 10.31305/rrijm.2021.v06.i03.002.
- [15] S. Haghbin, S. Lundmark, M. Alakula, and O. Carlson, "Grid-connected integrated battery chargers in vehicle applications: Review and new solution," *IEEE Trans. Ind. Electron.*, vol. 60, no. 2, pp. 459–473, 2013, doi: 10.1109/TIE.2012.2187414.
- [16] D. Howell, "Current Fiscal year (2012-2013) status of the hybrid and electric systems R&D at the U.S. - DOE," *World Electr. Veh. J.*, vol. 6, no. 3, pp. 502–513, 2013, doi: 10.3390/wevj6030502.
- [17] B. Singh, B. N. Singh, A. Chandra, K. Al-Haddad, A. Pandey, and D. P. Kothari, "A review of three-phase improved power quality ac-dc converters," *IEEE Trans. Ind. Electron.*, vol. 51, no. 3, pp. 641–660, 2004, doi: 10.1109/TIE.2004.825341.
- [18] B. Singh, B. N. Singh, A. Chandra, K. Al-Haddad, A. Pandey, and D. P. Kothari, "A review of single-phase improved power quality AC-DC converters," *IEEE Trans. Ind. Electron.*, vol. 50, no. 5, pp. 962–981, 2003, doi: 10.1109/TIE.2003.817609.
- [19] G. Y. Choe, J. S. Kim, B. K. Lee, C. Y. Won, and T. W. Lee, "A Bi-directional battery charger for electric vehicles using photovoltaic PCS systems," *2010 IEEE Veh. Power Propuls. Conf. VPPC 2010*, 2010, doi: 10.1109/VPPC.2010.5729223.
- [20] M. A. Fasugba and P. T. Krein, "Gaining vehicle-to-grid benefits with unidirectional electric and plug-in hybrid vehicle chargers," *2011 IEEE Veh. Power Propuls. Conf. VPPC 2011*, 2011, doi: 10.1109/VPPC.2011.6043207.
- [21] M. A. Fasugba and P. T. Krein, "Cost benefits and vehicle-to-grid regulation services of unidirectional charging of electric vehicles," *IEEE Energy Convers. Congr. Expo. Energy Convers. Innov. a Clean Energy Futur. ECCE 2011, Proc.*, pp. 827–834, 2011, doi: 10.1109/ECCE.2011.6063856.

- [22] H. Chen, X. Wang, and A. Khaligh, "A single stage integrated bidirectional AC/DC and DC/DC converter for plug-in hybrid electric vehicles," *2011 IEEE Veh. Power Propuls. Conf. VPPC 2011*, vol. 2, 2011, doi: 10.1109/VPPC.2011.6042980.
- [23] N. M. L. Tan, T. Abe, and H. Akagi, "Design and performance of a bidirectional isolated DC-DC converter for a battery energy storage system," *IEEE Trans. Power Electron.*, vol. 27, no. 3, pp. 1237–1248, 2012, doi: 10.1109/TPEL.2011.2108317.
- [24] X. Zhou, G. Wang, S. Lukic, S. Bhattacharya, and A. Huang, "Multi-function bi-directional battery charger for plug-in hybrid electric vehicle application," *2009 IEEE Energy Convers. Congr. Expo. ECCE 2009*, pp. 3930–3936, 2009, doi: 10.1109/ECCE.2009.5316226.
- [25] D. C. Erb, O. C. Onar, and A. Khaligh, "Bi-directional charging topologies for plug-in hybrid electric vehicles," *Conf. Proc. - IEEE Appl. Power Electron. Conf. Expo. - APEC*, pp. 2066–2072, 2010, doi: 10.1109/APEC.2010.5433520.
- [26] S. B. Peterson, J. F. Whitacre, and J. Apt, "The economics of using plug-in hybrid electric vehicle battery packs for grid storage," *J. Power Sources*, vol. 195, no. 8, pp. 2377–2384, 2010, doi: 10.1016/j.jpowsour.2009.09.070.
- [27] S. Bolognani, A. Faggion, and L. Sgarbossa, "Design of a flux weakening control scheme for DC motor drives featuring full voltage operation," *Proc. Univ. Power Eng. Conf.*, 2008, doi: 10.1109/UPEC.2008.4651658.
- [28] R. T. Naayagi, A. J. Forsyth, and R. Shuttleworth, "High-power bidirectional DC-DC converter for aerospace applications," *IEEE Trans. Power Electron.*, vol. 27, no. 11, pp. 4366–4379, 2012, doi: 10.1109/TPEL.2012.2184771.
- [29] X. Ruan, "Soft-Switching PWM Full-Bridge Converters: Topologies, Control, and Design," *Soft-Switching PWM Full-Bridge Convert. Topol. Control. Des.*, vol. 9781118702208, pp. 1–212, Jun. 2014, doi: 10.1002/9781118702215.
- [30] J. Han, X. Zhou, S. Lu, and P. Zhao, "A Three-Phase Bidirectional Grid-Connected AC/DC Converter for V2G Applications," *J. Control Sci. Eng.*, vol. 2020, 2020, doi: 10.1155/2020/8844073.
- [31] S. Piasecki, M. Jasiński, and A. Milicua, "Brief view on control of grid-interfacing AC-DC-AC converter and active filter under unbalanced and distorted voltage conditions," *COMPEL - Int. J. Comput. Math. Electr. Electron. Eng.*, vol. 30, no. 1, pp. 351–373, 2011, doi: 10.1108/03321641111091601.
- [32] W. Jiang and B. Fahimi, "Multiport Power Electronic Interface — Concept," *Power*, vol. 26, no. 7, pp. 1890–1900, 2011.

- [33] M. Michon, J. L. Duarte, M. Hendrix, and M. G. Simões, “A three-port bi-directional converter for hybrid fuel cell systems,” *PESC Rec. - IEEE Annu. Power Electron. Spec. Conf.*, vol. 6, pp. 4736–4742, 2004, doi: 10.1109/PESC.2004.1354836.

- [34] S. A. Khan, M. R. Islam, Y. Guo, and J. Zhu, “A New Isolated Multi-Port Converter With Multi-Directional Power Flow Capabilities for Smart Electric Vehicle Charging Stations,” *IEEE Trans. Appl. Supercond.*, vol. 29, no. 2, Mar. 2019, doi: 10.1109/TASC.2019.2895526.

- [35] Y. Zhang and D. Jiang, “A new coupled inductor structure with larger leakage inductance for EMI suppression,” *PEDG 2019 - 2019 IEEE 10th Int. Symp. Power Electron. Distrib. Gener. Syst.*, pp. 51–54, Jun. 2019, doi: 10.1109/PEDG.2019.8807781.

APPENDIX A

Full result of TAB system with same phase shift angle

Load (kW)	Shift Angle, θ (°)	Input Current (A)	Input Volt (V)	Input Power (kW)	Output Current Port 2 (A)	Output Voltage Port 2 (V)
100	0 : 90 : 90	241	452	106	121	471
	0 : 75 : 75	199	460	94	99	469
	0 : 60 : 60	203	459	75	111	441
	0 : 45 : 45	163	467	59	82	388
	0 : 25 : 25	170	466	47	85	266
75	0 : 40 : 40	113.9	474	54.6	63.8	465.7
	0 : 30 : 30	95	479	46	52	385.5
	0 : 25 : 25	82.9	471	40	71.6	348
	0 : 15 : 15	98.6	471.8	48.3	70	239
	0 : 10 : 10	114.5	466	56	83.8	171.8
50	0 : 25 : 25	78.5	485	38.1	39.3	495.7
	0 : 24 : 24	82	489	40	26.8	474.9
	0 : 20 : 20	63.5	478	31	53	415.8
	0 : 15 : 15	75	481	37	45	345
	0 : 10 : 10	93	474	45.8	64	247
25	0 : 11 : 11	35	492	17	19.4	487.9
	0 : 10 : 10	53.39	493.5	26	16.2	438.8
	0 : 9 : 9	53.4	493.5	26	16.2	438.8
	0 : 8 : 8	42.5	483	20	42	401
	0 : 5 : 5	66	477.9	32.5	55	307

Output Power Port 2 (kW)	Output Current Port 3 (A)	Output Voltage Port 3 (V)	Output Power Port 3 (kW)	Efficiency (%)
53	114	466	53	100
46	100	466	46	98
35	80	439	35	93
24	61	387	24	81
13	48	266	13	55
26.5	59.9	464.7	26.5	97
18.3	47.5	385.1	18.3	80
14	41.5	347	14	70
11.7	49	237	11.7	48
9.6	57.3	167.8	9.6	34
19	39.3	495	19	99.7
19.5	41	474.8	19.5	98
13.2	31.7	415.3	13.2	85
13	37.6	344	13	70
11	46.6	244.5	11	48
8	17.7	487.8	8	94
11.7	26.7	438	11.7	90
11	26.7	438	11	85
8.4	21	400	8.4	84
10	33	304.6	10	62

APPENDIX B

Full result of TAB system with various phase shift

Load (kW)	Shift Angle, ϕ (°)	I in (A)	V in (V)	P in (kW)	Io Port 2 (A)	Vo Port 2 (V)	Po Port 2 (kW)	Io Port 3 (A)	Vo Port 3 (V)	Po Port 3 (kW)	Efficiency (%)
100	0 : 90 : 75	222	455	101010	124	508	62992	88.5	419	37081.5	99
	0 : 90 : 60	230	453.6	104328	76.8	526.7	40450.56	83.7	341	28541.7	66
	0 : 90 : 45	219	456	99864	94.8	531	50338.8	58.9	258.9	15249.21	66
	0 : 90 : 25	227.6	454	103330	105.9	508.9	53892.51	60	116	6960	59
	0 : 90 : 0	247	450	111150	103.7	476	49361.2	88	7.4	651.2	45
	0 : 75 : 90	214	467	99938	88.5	419	37081.5	124	503	62372	100
	0 : 60 : 90	230	453.6	104328	76.8	526.7	40450.56	83.7	341	28541.7	66
	0 : 45 : 90	219	456	99864	94.8	531	50338.8	58.9	258.9	15249.21	66
75	0 : 25 : 90	227.6	454	103330	60	116	6960	105.9	508.9	53892.51	59
	0 : 0 : 90	247	450	111150	88	7.4	651.2	103.7	476	49361.2	45
	0 : 40 : 30	101	482	48682	84	488.7	41050.8	80	335	26800	139
	0 : 40 : 25	98	483.6	47392.80	69	499	34431	50	282	14100	102
	0 : 40 : 15	102.5	485	49712.50	77	493	37961	80	139.8	11184	99
	0 : 40 : 10	110.9	485	53786.50	74.9	481.8	36086.82	93.3	57.7	5383.41	77
	0 : 40 : 0	118	485	57230.00	74.3	470.7	34973.01	104	11	1144	63
	0 : 30 : 40	101	482.6	48742.60	80	335	26800	84.2	488.7	41148.54	139
50	0 : 25 : 40	98.2	483.6	47489.52	50	282	14100	69	499	34431	102
	0 : 15 : 40	102.5	485	49712.50	80	139.8	11184	77	493	37961	99
	0 : 10 : 40	110.9	485	53786.50	93	57.7	5366.1	74.9	481.8	36086.82	77
	0 : 0 : 40	118	485	57230.00	104	11	1144	74.3	470.7	34973.01	63
	0 : 25 : 8	81.8	488.8	39983.84	58.7	527.1	30940.77	84.7	116	9825.2	102
	0 : 25 : 7	86.98	488.6	42498.43	60.9	519.5	31637.55	94.8	79.1	7498.68	92
	0 : 25 : 6	86.9	488.6	42459.34	60.9	519.5	31637.55	94.8	79.1	7498.68	92
	0 : 25 : 5	90.7	488	44261.60	58.9	514.7	30315.83	97.8	52.8	5163.84	80
0 : 25 : 0	97.9	488	47775.20	59.9	505	30249.5	108.7	13	1413.1	66	
25	0 : 8 : 25	81.8	488.8	39983.84	84.7	116	9825.2	58.7	527.1	30940.77	102
	0 : 7 : 25	86.98	488.6	42498.43	94.8	79.1	7498.68	60.9	519.5	31637.55	92
	0 : 6 : 25	86.9	488.6	42459.34	94.8	79.1	7498.68	60.9	519.5	31637.55	92
	0 : 5 : 25	90.7	488	44261.60	97.8	52.8	5163.84	58.9	514.7	30315.83	80
	0 : 0 : 25	97.9	488	47775.20	108.7	13	1413.1	59.9	505	30249.5	66
	0 : 11 : 4	58.8	492.9	28982.52	39.9	518.8	20700.12	81.2	164.6	13365.52	118
	0 : 11 : 3	58.8	492.9	28982.52	39.9	518.8	20700.12	81.2	164.6	13365.52	118
	0 : 11 : 2	66	492	32472.00	36.7	517.8	19003.26	87	111	9657	88
	0 : 11 : 1	78.7	491.5	38681.05	38.6	505	19493	102.6	42.6	4370.76	62
	0 : 11 : 0	84.4	491.1	41448.84	38.3	499	19111.7	108.6	15.7	1705.02	50
	0 : 4 : 11	58.8	492.9	28982.52	81.2	164.6	13365.52	39.9	518.8	20700.12	118
	0 : 3 : 11	58.8	492.9	28982.52	81.2	164.6	13365.52	39.9	518.8	20700.12	118
0 : 2 : 11	66	492	32472.00	87	111	9657	36.7	517.8	19003.26	88	
0 : 1 : 11	78.7	491.5	38681.05	102.6	42.6	4370.76	38.6	505	19493	62	
0 : 0 : 11	84.4	491.1	41448.84	108.6	15.7	1705.02	38.3	499	19111.7	50	